Nature Inspired Metaheuristic Optimization Based Control Strategy for DC-DC Buck Converter



Researcher: Supervisor:

Uzma Shabbir Dr Suheel Abdullah Malik

171-FET/MSEE/F22

DEPARTMENT OF ELECTRICAL AND COMPUTER ENGINEERING FACULTY OF ENGINEERING AND TECHNOLOGY INTERNATIONAL ISLAMIC UNIVERSITY, ISLAMABAD May, 2025

Nature Inspired Metaheuristic Optimization Based Control Strategy for DC-DC Buck Converter



Uzma Shabbir

171-FET/MSEE/F22

This dissertation is submitted to Faculty of Engineering and Technology, International Islamic University Islamabad Pakistan for partial fulfillment of the degree of **MS Electrical Engineering** at Faculty of Engineering and Technology, Department of Electrical and Computer Engineering, International Islamic University, Islamabad.

Supervised By May, 2025

Dr Suheel Abdullah Malik

Declaration

Date:	Uzma Shabbir
been acknowledged properly.	
elsewhere for assessment. Moreover, the material take	en from other sources has also
Strategy for DC-DC Buck Converter" is my own wo	ork and has not been presented
certify that research "Nature Inspired Metaheuristic	COptimization Based Control

171-FET/MSEE/F22



In the name of Allah (SWT), the most beneficent and the most merciful

Dedicated

to

My caring parents, family and Respected Teachers

Certificate of Approval

This is to certify that the work contained in thesis entitled, "Nature Inspired Metaheuristic Optimization Based Control Strategy for DC-DC Buck Converter" was carried out by Ms. Uzma Shabbir, Registration No. 171-FET/MSEE/F22 and it is fully adequate in scopeand quality for the degree of MS Electrical Engineering.

Viva Voce Committee:

Supervisor	
Dr. Suheel Abdullah Malik	
Associate Professor, DECE, FET, IIU Islamabad	
External Examiner	
Dr	
Internal Examiner	
Dr	
Chairman DECE, FET, IIU Islamabad	
Dr. Ihsan ul Haq	
Associate Professor, DECE, FET, IIU Islamabad	
Dean FET, IIU Islamabad	
Dr. Saeed Badshah	
Professor DME, FET, IIU Islamabad	
May, 2025	

Abstract

DC-DC buck converter is type of power converter used to step down the level of output voltage. DC-DC buck converter is preferred over regulators due to its simple design and high efficiency. They are extensively used in many industrial and residential applications like solar inverters, grid tied inverter and power supplies. Non-linear characteristics of buck converter introduce periodic changes in its output voltage and if not regulated can ultimately lead to instability which makes the device sensitive to even small changes in the parameters of circuits. Keeping in view the diverse real-life applications of buck converter two controllers has been designed in this thesis for voltage regulation of buck converter. The two controllers PID and modified version of PID that is I-PD is optimally tuned by using three metaheuristic optimization techniques: Grey Wolf Optimization (GWO), Jellyfish Search Optimization (JSO), and Fitness Dependant Optimization (FDO). The efficiency of the optimized controllers has been determined with four standard performance criteria that are widely used in practice, named as IAE, ISE, ITAE, and ITSE. The indices are used to analyze transient and steady-state performances of the systems, thus giving a complete picture of the controller performance. Two separate cases of converter are considered here with different parameters. Consequently, the analysis of the outcome shows that the proposed optimization algorithms considerably improves the PID and I-PD controllers' transient response, steady-state accuracy, system robustness, and dynamic stability.

Acknowledgment

With the blessings of Allah (S.W.T), I humbly offer my gratitude for the guidance

and support received during the completion of this research. May peace and blessings

be upon the last Prophet Hazrat Muhammad (S.A.W) and all his companions (R.A),

who devoted their livesto the prosperity and spread of Islam.

I am truly obliged for the instrumental support provided by my supervisor, Dr. Suheel

AbdullahMalik. Without his support, encouragement, and unwavering patience, this

dissertation would not have been possible. He provided the guidance and motivation

needed to see this project through to completion, and I am deeply thankful for his

contributions.

May Allah grant us the wisdom to follow the teachings of the Holy Qur'an and Sunnah

in all aspects of our lives.

Uzma Shabbir

Date: ______ 171-FET

171-FET/MSEE/F22

viii

Table of Contents

Declaration	iii
Certificate of Approval	V
Abstract	vii
Acknowledgement	viii
Table of Contents	9
List of Figures	14
List of Tables	16
Chapter 1 Introduction	17
1.1. Overview	17
1.2. Problem Statement	18
1.3. Research Objectives	19
1.4. Significance of Research	19
1.5. Composition of thesis	20
Chapter 2 Literature Review	21
2.1 Previous Work	21

Chapter 3 Modeling of DC-DC Buck Converter and Controllers Design30
3.1. Overview
3.2. Mathematical model of DC-DC Buck Converter
3.3. Controllers
3.3.1. PID Controller
3.3.2. I-PD Controller
3.4. Evolutionary Computing Techniques41
3.4.1. Grey Wolf Optimization Algorithm (GWO)41
3.4.2. Jellyfish Search Optimization Algorithm (JSO)44
3.4.3. Fitness Dependent Optimization Algorithm (FDO)
Chapter 4 Formulation of Objective Function and Performance Indices50
4.1. Objective Function
4.2. Derivation of Error for PID and I-PD controller
4.3. Case I50
4.3.1. Derivation of Error for PID controller
4.3.2. Derivation of Error for I-PD controller
4.4. Case II

4.4.1.	Derivation of Error for PID controller	52
4.4.2.	Derivation of Error for I-PD controller	53
4.5. P	erformance Indices	53
4.5.1.	Integral of absolute value of error (IAE)	54
4.5.2.	Integral of square error (ISE)	54
4.5.3.	Intergal of time multiplied by absolute value of error (ITAE)	54
4.5.4.	Integral of time multiplied by squared value of error (ITSE)	54
Chap	ter 5 Implementation and Results	56
5.1.	Step response for DC-DC buck converter for Case-I and Case-II without ontroller	56
5.2.	Perameters Setting for GWO, JSO and FDO	57
5.3.	Case I	57
5.3.1.	Control parameters of GWO-PID, JSO-PID, and FDO-PID controllers	58
5.3.2.	Control parameters of GWO-I-PD, JSO-I-PD, and FDO-I-PD controllers	58
5.3.3.	Step response of GWO-PID, JSO-PID, and FDO-PID controllers	59
5.3.4.	Performance comparison of GWO-PID, JSO-PID, and FDO-PID controllers	60
5.3.5.	Step response of GWO-I-PD, JSO-I-PD, and FDO-I-PD controllers	61

5.3.6 Performance comparison of GWO-I-PD, JSO-I-PD, and FDO-I-PD controllers	.62
5.3.7. Performance comparison of proposed controllers with reference papers	.63
5.4. Case II	.64
5.4.1. Control parameters of GWO-PID, JSO-PID, and FDO-PID controllers	.64
5.4.2. Control parameters of GWO-I-PD, JSO-I-PD, and FDO-I-PD controllers	.65
5.4.3. Step response of GWO-I-PD, JSO-I-PD, and FDO-I-PD controllers	.66
5.4.4. Performance comparison of GWO-PID, JSO-PID, and FDO-PID controllers	.67
5.4.5. Step response of GWO-I-PD, JSO-I-PD, and FDO-I-PD controllers	.68
5.4.6. Performance comparison of GWO-I-PD, JSO-I-PD, and FDO-I-PD controllers	.69
5.4.7. Performance comparison of proposed controllers with reference papers	.70
6. Conclusion and Future Work	.72
6.1. Conclusion	.72
6.2. Future Recommendations	.73
References	.75
Appendix A	.81
Annondiv D	Q2

Appendix C	85
11	
Appendix D	87

List of Figures

Figure 3.1: (a) DC-DC buck converter; (b) Equivalent circuit when MOSFET switch is
ON; (c) Equivalent circuit when MOSFET switch is OFF
Figure 3.2: Structure of PID controller
Figure 3.3: Control structure of PID controller for Case-I
Figure 3.4: Control structure of PID controller for Case-II
rigure 5.4. Control structure of 1 1D controller for Case-II
Figure 3.5: I-PD controller structure
Figure 3.6: Control structure of I-PD controller for Case-I
Figure 3.7: Control structure of I-PD controller for Case-II
Figure 3.8: Flow chart for GWO
1 igure 0.0.1 iow chair ioi o w o
Figure 3.9: Flow chart of JSO
Figure 3.10: Flow chart of FDO.
Element 4.1. Control structure for DID and a 11 or for Cons. I
Figure 4.1: Control structure for PID controller for Case-I
Figure 4.2: Control structure for I-PD controller for Case-I
Figure 4.3: Control structure for PID controller for Case-II

Figure 4.4: Control structure for I-PD controller for Case-II	53
Figure 5.1: Step response for Case-I	56
Figure 5.2: Step response for Case-II	57
Figure 5.3: Step response of DC-DC Buck Converter System with GWO-PID, JS and FDO-PID controllers for Case-I	
Figure 5.4: Step response of DC-DC Buck Converter System with GWO-I-PD, JS and FDO-I-PD controllers for Case-I	
Figure 5.5: Step response of DC-DC Buck Converter System with GWO-PID, JS and FDO-PID controllers for Case-II	
Figure 5.6: Step response of DC-DC Buck Converter System with GWO-I-PD, JS and FDO-I-PD controllers for Case-II	

List of Tables

Table 2.1: Concise Overview of Literature review 26
Table 3.1: Different parameters for Case-I 36
Table 3.2: Different Parameters for Case-II
Table 5.1: Parameters setting for GWO,JSO and FDO 57
Table 5.2: Control Parameters of GWO-PID, JSO-PID, and FDO-PID controllers58
Table 5.2: Control Parameters of GWO-I-PD, JSO-I-PD, and FDO-I-PD controllers59
Table 5.3: Performance comparison of GWO-PID, JSO-PID and FDO-PID controllers61
Table 5.4: Performance comparison of GWO-I-PD,JSO-I-PD and FDO-I-PD controllers 63
Table 5.5: Performance comparison of proposed controller with reference papers64
Table 5.6: Control Parameters of GWO-PID, JSO-PID, and FDO-PID controllers65
Table 5.7: Control Parameters of GWO-I-PD,JSO-I-PD and FDO-I-PD controllers66
Table 5.8: Performance comparison of GWO-PID, JSO-PID and FDO-PID controllers68
Table 5.9: Performance comparison of GWO-I-PD, JSO-I-PD and FDO-I-PD controllers
Table 5.10: Performance comparison of proposed controller with reference papers71

Chapter 1 Introduction

1.1. Overview

Power converters are involved in performing essential and revolutionary tasks in different electrical energy applications. These converters are very much used in diverse residential, industrial and commercial applications like the grid-tied inverters, solar inverters and power supplies. They are considered vital component in various renewable and conventional energy systems due to their ability to manage electrical energy efficiently. In the class of power converters, the DC to DC buck converter is one of the most utilized power electronic systems due to its higher voltage conversion efficiency and flexibility in providing output voltage that is adjustable. This makes it suitable in many applications including voltage regulation, and energy efficient voltage conversion [1]. Also, it is small in size and operates with high efficiency than conventional voltage regulators and thus used widely in industrial applications and consumer electronics.

However, the DC-DC buck converter has inherent problems because of its non-linear topology in steady-state operation. These non-linearities cause periodic fluctuations in the output voltage and if not regulated can ultimately lead to instability. Such fluctuations of output voltage make the converter very sensitive to changes in the circuit parameters and therefore complex control methods have to be employed to ensure its stability. Consequently, accurate control of the voltage at output is desirable, particularly for a wide range of load fluctuations or disturbances in the input source.

To deal with these challenges, researchers have come up with several controller designs with an intention of improving the DC-DC buck converters performance. The most popular among the process controllers are the classical PID controllers and their derived forms, which are created to minimize the steady-state errors and enhance the dynamic performance of the system. These controllers operate by 'tuning' the converter in real time to achieve a constant output voltage, capable of modifying according to given circumstances [2]. The enhancement of these controllers is still an active area because they give the application a way to improve the converter performance to reduce energy loss and control the system behavior in different conditions.

To deal with the different challenges of buck converter, this thesis investigates PID and I-PD controller with different optimization algorithms such as Grey Wolf Optimization (GWO), Jellyfish Search Optimization (JSO), and Fitness Dependent Optimization (FDO) to optimize the controller performance, ability to regulate output voltage effectively and efficiently. This thesis aims to minimize the error indices so that overall efficiency of buck converter will be improved and thereby contributing to the advancement of power electronics for energy management applications.

1.2. Problem Statement

Due to the non-linear behavior and fast dynamics of the DC-DC buck converter, output voltages deviate from the desired value. This makes the device sensitive to even small changes in the parameters of the circuit. The change in the output voltage of the DC-DC converter will lead to the failure of load operation. So, the voltage regulation issue of the DC-DC buck converter cannot be ignored. Although several different controllers have been proposed to eliminate the mismatch between the output voltage and the set point of the DC-DC buck converters, however, it still is a challenging task to design efficient controllers with adequate speed while maintaining the stability of the output voltage.

The objective of this research is to address these challenges by designing and optimizing nature inspired metaheuristics based controllers for DC-DC buck converter system. The study aims to model DC-DC buck converter system, formulate fitness functions, and optimizes the PID and modified form of PID (I-PD) controller using three nature inspired metaheuristics algorithms, namely, GWO, JSO, and FDO. The performance of the proposed controllers will be evaluated using four performance indices such as ITSE, ISE, IAE, and ITAE.

1.3. Research Objectives

- 1. Modeling of DC-DC buck converter.
- Modeling and Design of PID and I-PD controllers for two distinct cases of DC-DC buck converter.
- Formulation of fitness function and Optimization of fitness function using three nature inspired metaheuristic optimization techniques that are Grey Wolf Optimization Algorithm, Jellyfish Search Optimization Algorithm and Fitness Dependent Optimization Algorithm.
- 4. Performance evaluation of proposed controllers using four performance indices IAE, ISE, ITAE and ITSE.

1.4. Significance of Research

This research will have a far-reaching impact across multiple industries involved in power electronic converters, switching power supplies, mobile industries, etc. operation and control. The chosen system is used in renewable energy integration systems like grid-tied inverters, renewable energy utilization systems like solar inverters and wind turbines, telecommunication systems like networking equipment, and aerospace defense systems. So, this research will result in the development of advanced control techniques that will help in

better reliability, stability, and efficiency of DC-DC buck converters in these systems.

1.5. Composition of Thesis

The thesis report has been ordered in the five chapters. The brief summary is given below:

Chapter 1: It is about the problem introduction and some basic knowledge of the DC-DC buck converter. It covers the significance of the research.

Chapter 2: Concise overview of literature review is given.

Chapter 3: It is about basic knowledge of DC-DC buck converter, modeling of system for two distinct cases with different parameters and summary of 3 main used heuristic algorithms.

Chapter 4: It is about formulation of fitness function for GWO-PID, JSO-PID, FDO-PID, and GWO-I-PD, JSO-I-PD, and FDO-I-PD controllers for both cases.

Chapter 5 is about the implementation of proposed controllers and discussion of results obtained.

Chapter 6 is about the conclusion of research work it also recommends some techniques for the future work in the same problem area.

Chapter 2 Literature Review

This chapter contains the brief summary of different proposed controllers and optimization techniques for voltage regulation of DC-DC buck converter.

2.2. Previous Work

DC-DC converters are extensively used in many of the residential and industrial applications in grid connected inverters, solar inverters and power supplies. The high efficiency of this voltage regulator makes it popular in many devices. Buck converter's non linear characteristics caused the periodic changes in the output voltage to make this device sensitive to even small changes in parameters of the circuit. There has been a lot of research carried out due to the fact, that power electronic converters have numerous real life applications. So, an attempt of settled efforts has been made in designing robust and optimal controllers for DC-DC buck converter.

Voltage regulation of the buck converter using fractional order proportional integral derivative controller has been proposed by Izci and Ekinchi [3]. Improved version of hunger game search algorithm was developed with the help of Randomized Local Search (RLS) and Nelder Mead Simplex (NMS). This algorithm was tested for several bench mark functions that are unimodal, fixed dimension and multimodal in nature. An improved objective function by modifying the structure of ISE was proposed. The Comparison was made with other recent metaheuristic methods such as HGS-FOPID, HHO-FOPID, LFD-PIDA, and AEO-PID, and the better transient and frequency response, superiority in robustness and disturbance rejection, as well as in the load handling capacity of the proposed method, was depicted [3]. The authors [4] proposed a cascaded controller PD (I+PI) due to responsive mode of buck converter. They observed that when multistage PD controller is connected to (I+PI) controller

in cascade form, the response is much better than the traditional controllers like PID and FOPID. The proposed controller parameters were optimized by using Mayfly Optimization Algorithm and the results show reduction in settling time and rise time.

Hekimoglu and Ekindhi [5] proposed a hybrid algorithm by using Simulating Annealing and Whale Optimization Algorithm. The application of the proposed algorithm results in acquisition of the parameters of the PID controller. It is then verified with a time domain performance index that means the settling time, rise time, and overshoot of the buck converter reduce with other controllers such as the SA-PID, etc. [5].

Izci et al, in [6] designed Artificial Ecosystem based optimization intergrated with Nelder Mead (AEONM), which is hybrid algorithm which combines Artificial Ecosystem based optimization with Nelder Mead. The proposed algorithm successfully obtained the parameter of PID controller. The AEONM Algorithms was tested on some main functions such as Ackley function, buck converter function, and was compared with PSO and DE algorithms. AEONM showed better performance. The performance analysis conducted on the designed AEONM system showed better performance of the method over others and overall disturbance rejection capability.

The authors [7] proposed PID controller and optimized its parameter by using Archimedes Optimization Algorithm. For buck converter, AOA was used to find out the best PID controller parameters and comparison with other algorithms like AEONM, AEO, DE, and PSO showed an improvement in transient and somewhat reducing performance degradation in case of load change.

Buck converter's voltage regulation is absolutely essential, as the deviation of output voltage from the designated one may lead to the failure of the load, as discussed by the authors [8].

The author used ICSA for finding the parameters of proposed controller (PID). Other types of controller SC-PID, AEONM-PID, PSO-PID, DE-PID were compared with the obtained results in terms of their transient response characteristics and disturbance rejection.

The parameters of the controller used in Voltage regulation controller for the buck converter have been optimized by using an Improved Differential Evolution algorithm proposed Zhao et al.[9]. The proposed method reduced regulation time, rise time and no oscillation in the system's dynamic performance was observed.

Alfergani et al. [10] proposed PI controller for buck converter and the controller parameters have been optimally obtained by using genetic algorithm. The author proposed four different performance indices ITSE, ISE, ITAE and ITSE as objective function. The controller was tuned for each performance indices and results were compared for four performance indices. Obtained results revealed that ITSE gives superior performance as compared to other objective functions. Fuzzy PID control technique named as PSO control technique with chaos variables for a buck converter has been proposed by Zou and Xue [11]. Besides, the approach used was found to outperform the PID and fuzzy PID control strategies particularly in the aspect of adjustment time, system overshoot and robustness under dynamic as well as steady-state operating condition.

Warrier and Shah [12] proposed FOPID controller and new metaheuristic algorithm, CI, meant for tuning the parameters of the proposed controllers. CI was tested for four performance indices as objective function for proposed controller and the obtained results showed the superior performance of ISE performance indices. Also the obtained results was compared with other metaheuristics algorithms PSO, GA, ABC and SA, and it showed that CI-FOPID controller gives comparable results at a much faster rate. The author in [13]

proposed ABC optimization algorithm based PID controller for a buck converter. The proposed model was tested in MATLAB to verify its effectiveness, subjecting it to various forms of input disturbance, such as sudden changes in input and output voltages, as well as fluctuations in the load resistance.

In [14], the author proposed BOA based PID controller for voltage regulation of step down converter used for mobile applications. The proposed algorithms was used to find out the best parameters and simulated result was compared with Self tuning PID and DEO algorithm and proposed method showed better response in terms of reduce rise and settling time and reduce rise of the plant. The system also showed steady response when load resistance was varied, which minimized the rise time and settling time and improved the transient as well as steady state responses as compared to other controlling systems. A fractional order fuzzy based PID controller has been proposed by Ghamari et al. [15] to control a buck converter, where PID controller was tuned using ALO algorithm. Then, this method was compared to PSO-PID and fractional order PID controller. The result obtained showed that the performance is good in speed and effectiveness to noise perturbation and load changes. It was seen that the ALO algorithm always performs better than the general form of the optimization methods since the efficiency of the controller increases.

Filho et al. [16] proposed PID controller and controller parameters were obtained by using 10 variations of bio inspired optimization algorithms. The obtained results for all the used optimization techniques were compared using fitness function values. Comparison shows that DE and PSO showed superior performance as DE and PSO variants have highest value of fitness function.

For buck converter, Bakria et al. [17] proposed SH optimization algorithm to optimize PID controller. The proposed control method was implemented in MATLAB and the obtained results showed disturbance rejection and enhanced systems dynamics. In [18] authors proposed a hybrid algorithm named as CFP algorithms based on chaos theory with different maps and flower pollination algorithm. The optimal PID controller was compared with FOA and WOA and shows better performance in terms of lower value of ISE.

Nishat et al. [19] proposed GA-based-PID controller to test stability of close loop buck converter. The comparative analysis indicated that GA-PID controller response was indeed optimized for several parameters. When results were compared, the GA-based PID controller presented a better dynamic stability and efficiency than other tuning methods to select for the buck converter application. Debnath et al. [20] obtained optimal control parameters of PID controller through the application of a PSO based optimization. The method effectively reduced cost functions including ISE, IAE, ITSE, and ISTSE and accurately determines the controller parameters improving the converter's performance under load and voltage variation. Author in [21] used GA-PID controller for regulating voltage of buck converter. The author used four performance indices ISE, MSE, IATE and IAE. The results were compared for all four performance indices and it shows that MSE gives superior performance. The author in [22] proposed FOPID controller for buck converter. He used ALO algorithm to tune the controller. The results were compared with PSO-PID and PSO-FOPID controller. The transient response characteristics showed that ALO-FOPID performed better than PSO-PID and PSO-PID controller.

Daraz in [23] proposed improved structure of I-PD for automatic generation control of multisource power system with non-linearity and optimizes the gain parameters using FDO. The obtained results showed superior performance when compared with other techniques like FA, PSO, and TLBO algorithm in term of O_{sh},U_{sh} and T_s. Daraz et al. in [24] proposed FDO algorithm to optimize gains of I-PD controller for same system as given above. The proposed controller was compared with LUS-PID, TLBO-PID and DE-PID, the results showed FDO-PID controller better results in term of O_{sh},U_{sh} and T_s. In [25] author proposed GWO algorithm for PI-PD controller gains optimization for unstable time delay system. The Controller proposed was implemented for three different models and compared with Darsi and Yin methods. The results showed superior performance of GWO for proposed controller for all three systems. Table 2 provides a concise overview of the literature review.

From the summary of literature review given in above paragraphs, it is concluded that the latest research [3]-[25] has been directed towards designing of efficient controller with adequate speed for voltage regulation of DC-DC buck converter. However, it is still a challenging task to design efficient and fast controller while maintaining stability of system. Despite existing efforts, optimization of controllers to enhance system dynamics needs further investigation.

This research addresses the need for more efficient and faster voltage regulation of DC-DC buck converters by designing and optimizing PID and I-PD controllers.

Table 2.1: Concise Overview of Literature review

Ref #.	Year	Controller	Tuning Algorithm	System	
[3]	2022	FOPID	HGS, IHGS	DC-DC	Buck
				Converter	
[4]	2022	PD(1+PI)	MOA	DC-DC	Buck

				Converter
[5]	2020	PID	Hybrid WOA	DC-DC Buck
				Converter
[6]	2021	PID	Artificial	DC-DC Buck
			Ecosystem based	Converter
			Optimization	
			integrated with	
			Nelder-Mead	
			method	
[7]	2023	PID	AOA	DC-DC Buck
				Converter
[8]	2024	PID	ISCA	DC-DC Buck
				Converter
[9]	2021	PID	Differential	DC-DC Buck
			Evolution	Converter
[10]	2023	PI	Genetic Algorithm	DC-DC Buck
				Converter
[11]	2023	Fuzzy PID	Particle Swarm	DC-DC Buck
			Optimization	Converter
[12]	2021	FOPID	Cohort Intelligence	DC-DC Buck
			Algorithm	Converter
[13]	2021	PID	Artificial Bee	DC-DC Buck
			Colony	Converter

[14]	2020	Adaptive PID	Bat Optimization	DC-DC Buck
			Algorithm	Converter
[15]	2021	FOPID	Ant lion	DC-DC Buck
			Optimization	Converter
			Algorithm	
[16]	2022	PID	Genetic Algorithm,	DC-DC Buck
			Differential	Converter
			Evolution, Particle	
			swarm optimization	
[17]	2021	PID	Spotted Hyenna	DC-DC Buck
			Optimizer	Converter
[18]	2021	PID	Chaotic Flower	DC-DC Buck
			Pollination	Converter
[19]	2020	PID	Genetic Algorithm	DC-DC Buck
				Converter
[20]	2021	PID	Particle Swarm	DC-DC Buck
			Optimization	Converter
[21]	2020	PID	Genetic Algorithm	DC-DC Buck
				Converter
[22]	2022	FOPID	Ant lion Optimizer	DC-DC Buck
			Algorithm	Converter
[23]	2020	I-PD	Fitness Dependent	Automatic
			Optimizer	Generation

				Control of
				Multisource
				Interconnected
				power system
[24]	2020	I-PD	Fitness Dependent	Automatic
			Optimizer	Generation
				Control of
				two Multisource
				Interconnected
				power system
[25]	2022	PI-PD	Grey Wolf	Unstable Cascade
			Optimizer	Processes

Chapter 3 Modeling of DC-DC Buck Converters and Controllers Design

3.1. Overview

The DC-DC converter is one of an important type from 4 types of power converter it convert DC of a certain voltage level to another voltage level. It can either be utilized to decrease or increase the amount of voltage. Few of the applications include grid-tie inverters, renewable energy utilization applications comprising solar inverters and windmills, and a lot of other electronic products like networking equipment and power supplies.

It has four main types and all types are used in several applications. Out of these four types, there is DC-DC buck converter, which has a lot of use and is used to decrease voltage level from one level to other. A DC-DC boost converter is a type that plays the role of the conversion of a lower voltage to a higher voltage. One of its applications is where the load demands an output voltage opposite to the input voltage. Standalone converters is another type that are always used in circuit where circuits where voltage at the output has to be electrically different from that at the input.

First type which is discussed in above discussion is buck converter and it is one of the specialized power converters with a capacity to reduce the output of the supplied input [26]. The supplied voltage is converted to specific level of output voltage at output with respect to the time-based pulse width modulation duty cycle. Since it is a step-down converter, then the level of voltage at the output side will always be less than the level of voltage at the input side.

3.2: Mathematical Model of DC-DC Buck Converter

It consists of a low-pass filter and a switch placed after the filter. The low-pass filter is based on an L and C. Figure 3.1 displays; a switching device is used in the circuit to alternately turn the device on and off. The switch is a solid-state component called a MOSFET, and PWM signal control it. Figure 3.1(b) display the buck converter equivalent circuit, when state of switch is on. When switch is in off state, the diode is in reverse biase condition and opens, allowing flow of current due to the input voltage. In Figure 3.2(c), the diode is short-circuited means it is in forward bias condition, allowing current flow due to the stored inductor energy. The circuit diagrams for converter, both with the switch ON and OFF, are shown in Figure 3.1.

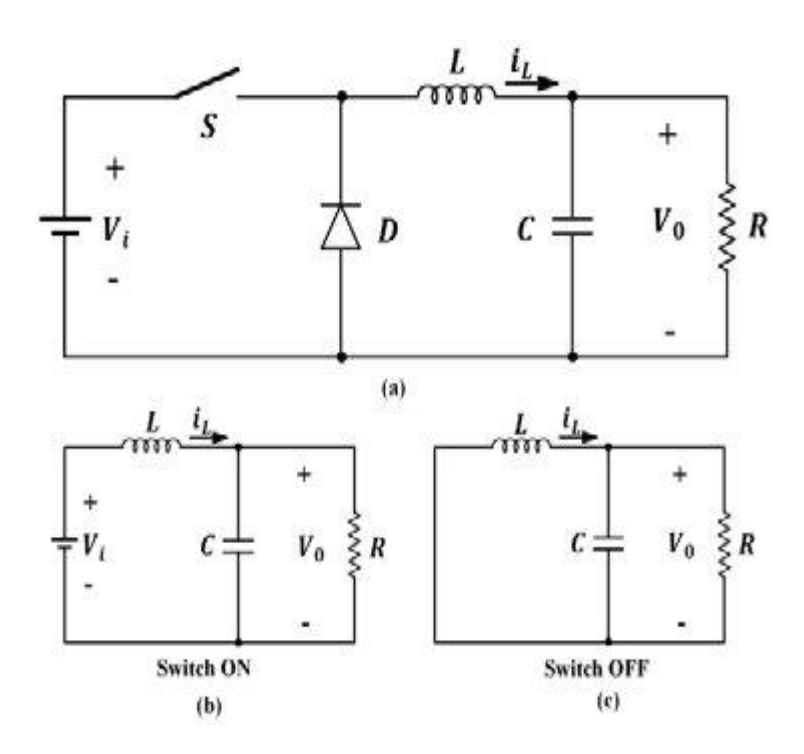


Figure 3.1: (a) DC-DC buck converter; (b) Equivalent circuit when MOSFET switch is ON; (c) Equivalent circuit when MOSFET switch is OFF [27]

Switch ON

From Figure 3.1(b) if we write the current voltage relationship for inductor then it can be written as [28].

$$V_{L} = \frac{L \, di_{L}(t)}{dt} = V_{i} - V_{0} \tag{3.1}$$

Rearranging equation 3.1

$$\frac{\operatorname{di}_{L}(t)}{\operatorname{dt}} = \frac{V_{i} - V_{0}}{L} \tag{3.2}$$

Again rearranging equation 3.2

$$\frac{\operatorname{di}_{L}(t)}{\operatorname{dt}} = \frac{V_{i}}{L} - \frac{V_{o}}{L} \tag{3.3}$$

Writing equation for inductor current from figure 3.1(b)

$$i_{L} = i_{o} - i_{c=} \frac{V_{o}}{R} + C \frac{dV_{o}}{dt}$$
 (3.4)

Rearranging equation 3.4

$$\frac{\mathrm{dV_0(t)}}{\mathrm{dt}} = \frac{\mathrm{i_L}}{\mathrm{C}} - \frac{\mathrm{V_0}}{\mathrm{RC}} \tag{3.5}$$

Switch OFF

From Figure 3.1(c) if we write the current voltage relationship for inductor then it can be written as [27].

$$V_{L} + V_{O} = 0 (3.6)$$

Rearranging equation 3.6

$$L\frac{di_{L}(t)}{dt} = -V_{o} \tag{3.7}$$

Writing current voltage relationship for capacitor then it can be written as

$$i_0 = i_L - i_c \tag{3.8}$$

$$i_c = i_o - i_L$$
 (3.9)

$$C\frac{dV_0}{dt} = \frac{V_0}{R} - i_L \tag{3.10}$$

$$\frac{\mathrm{d}V_{\mathrm{o}}(t)}{\mathrm{d}t} = \frac{V_{\mathrm{o}}}{C} - \frac{\mathrm{i}_{\mathrm{L}}}{C} \tag{3.11}$$

Writing equation 3.3 and 3.5 in matrix form

$$\begin{bmatrix}
\frac{di_L}{dt} \\
\frac{dv_o}{dt}
\end{bmatrix} = \begin{bmatrix}
0 & -\frac{1}{L} \\
\frac{1}{C} & -\frac{1}{RC}
\end{bmatrix} \begin{bmatrix}
i_L \\
V_o
\end{bmatrix} + \begin{bmatrix}
i \\
L \\
0
\end{bmatrix} V_i$$
(3.12)

Writing equation 3.7 and 3.10 in matrix form

$$\begin{bmatrix} \frac{\mathrm{di}_{L}}{\mathrm{dt}} \\ \frac{\mathrm{dv}_{o}}{\mathrm{dt}} \end{bmatrix} = \begin{bmatrix} 0 & -\frac{1}{L} \\ \frac{1}{C} & -\frac{1}{RC} \end{bmatrix} \begin{bmatrix} i_{L} \\ V_{o} \end{bmatrix} + \begin{bmatrix} 0 \\ 0 \end{bmatrix} V_{i}$$
 (3.13)

Equation 3.12 and 3.13 gives that there are two variables i_L and V_o , to write state space equations, assume

$$\mathbf{x}_1 = \mathbf{i}_{\mathbf{L}} \tag{3.14}$$

$$x_1' = \frac{di_L}{dt} \tag{3.15}$$

$$x_2 = V_o \tag{3.16}$$

$$x_2' = \frac{dV_o}{dt} \tag{3.17}$$

$$x' = Ax + Bu \tag{3.18}$$

To write average value for A matrix

$$A = A_{ON}D + A_{OFF}(1 - D)$$
 (3.19)

Using value of A_{ON} and A_{OFF} from equation 3.12 and 3.13 in equation 3.19

$$A = \begin{bmatrix} 0 & -\frac{1}{L} \\ \frac{1}{C} & -\frac{1}{RC} \end{bmatrix} d + \begin{bmatrix} 0 & -\frac{1}{L} \\ \frac{1}{C} & -\frac{1}{RC} \end{bmatrix} (1 - d)$$
 (3.20)

$$A = \begin{bmatrix} 0 & -\frac{1}{L} \\ \frac{1}{C} & -\frac{1}{RC} \end{bmatrix}$$
 (3.21)

Similarly, to write average value for B matrix

$$B = B_{ON}D + B_{OFF}(1 - D)$$
 (3.22)

Using value of B_{ON} and B_{OFF} from equation 3.12 and 3.13 in equation 3.22

$$B = \begin{bmatrix} \frac{1}{L} \\ 0 \end{bmatrix} d + \begin{bmatrix} 0 \\ 0 \end{bmatrix} (1 - d)$$
 (3.23)

$$B = \begin{bmatrix} \frac{d}{L} \\ 0 \end{bmatrix} \tag{3.24}$$

Put equation 3.21 and 3.24 in equation 3.18,

$$x' = \begin{bmatrix} 0 & -\frac{1}{L} \\ \frac{1}{C} & -\frac{1}{RC} \end{bmatrix} \begin{bmatrix} i_L \\ V_0 \end{bmatrix} + \begin{bmatrix} \frac{d}{L} \\ 0 \end{bmatrix} V_i$$
 (3.25)

Put equation 15 and 17 in equation 3.25

$$\begin{bmatrix} \frac{\mathrm{di}_{L}}{\mathrm{dt}} \\ \frac{\mathrm{d}V_{o}}{\mathrm{dt}} \end{bmatrix} = \begin{bmatrix} 0 & -\frac{1}{L} \\ \frac{1}{C} & -\frac{1}{RC} \end{bmatrix} \begin{bmatrix} i_{L} \\ V_{o} \end{bmatrix} + \begin{bmatrix} \frac{\mathrm{d}}{L} \\ 0 \end{bmatrix} V_{i}$$
 (3.26)

Taking Laplace transform of equation 3.26

$$s \begin{bmatrix} i_{L} - i_{L}(0) \\ V_{0} - V_{0}(0) \end{bmatrix} = \begin{bmatrix} 0 & -\frac{1}{L} \\ \frac{1}{C} & -\frac{1}{RC} \end{bmatrix} \begin{bmatrix} i_{L} \\ V_{0} \end{bmatrix} + \begin{bmatrix} \frac{d}{L} \\ 0 \end{bmatrix} V_{i}$$
 (3.27)

By considering $i_L(0) = 0$ and $V_o(0) = 0$, writing equation for

 i_L and V_o from equation 3.27

$$\operatorname{si}_{\mathrm{L}} = -\frac{\mathrm{V}_{\mathrm{o}}}{\mathrm{L}} + \frac{\mathrm{V}_{\mathrm{i}}\mathrm{D}}{\mathrm{L}} \tag{3.28}$$

$$sV_{o} = \frac{1}{C}i_{L} - \frac{V_{o}}{RC}$$
 (3.29)

Rearranging equation 3.29

$$sV_0 + \frac{V_0}{RC} = \frac{1}{C}i_L$$
 (3.30)

$$sC\left(sV_{o}\left(s\right) + \frac{V_{o}\left(s\right)}{RC} = si_{L}\right)$$
(3.31)

Putting equation 3.28 in equation 3.31

$$sC\left(sV_o(s) + \frac{V_o(s)}{RC} = -\frac{V_o}{L} + \frac{V_iD}{L}\right)$$
 (3.32)

Rearranging equation 3.32

$$V_o(s)\left(s^2C + \frac{s}{RC} = -\frac{V_o}{L} + \frac{V_iD}{L}\right)$$
 (3.33)

Further rearranging equation 3.33, buck converter transfer function will be as given in equation 3.34.

$$\frac{V_0(s)}{D(s)} = \frac{V_s}{LCs^2 + \frac{L}{R}s + 1}$$
 (3.34)

By putting the different values of different parameters in equation 3.34, different transfer function can be obtained. In this research, for first case, the values of different parameters as given in equation 3.34 have been used from table 3.1. The resultant expression is given in equation 3.35. This expression is used in case-I. Similarly to obtain the second expression for equation 3.34, parameters of table 3.2 are used and the obtained equation is given in equation 3.36. This expression is used in case-II.

Table 3.1: Different parameters for Case-I [3]

Voltage 36(V)
sistance $6(\Omega)$
ductor 1(mH)
pacitor 100(uF)
(

$$\frac{V_0(s)}{D(s)} = \frac{216000}{0.0006s^2 + s + 6000}$$
 (3.35)

Transfer function given in equation 3.35 and equation 3.36 are used in case-I and Case-II of this thesis respectively.

Table 3.2: Different parameters for Case-II [9]

Parameters	Definition	Values
Vi	Input Voltage	400(V)
R	Resistance	$8(\Omega)$
L	Inductor	1(<u>mH</u>)
C	Capacitor	10(uF)

$$\frac{V_o(s)}{D(s)} = \frac{1280}{8e - 8s^2 + 0.001s + 8}$$
 (3.36)

Efficient power conversion of buck converter makes them suitable for smaller gadgets due to less heat production and extended battery life. They are mostly used in power supplies that are switched mode, where the output voltage required is less than the voltage given at input.

Due to non linear behavior and fast system dynamics their control is difficult. The controller is designed to remove the e ss and improving the system dynamics of converter. Introduction of MOSFET has resulted in high speed dynamics of the system.

3.3. Controllers

Controller is a device that is used to regulate the system behaviors by adjusting its inputs to achieve desired output. System current state is continuously measured by controller through sensor and based on difference between set point and actual state adjustments are made in controller gains to obtain the desired output. In this research, two controllers have been implemented for buck converters that are PID and I-PD controller. PID controller is defined as integration of three controllers named as P, D and I connected in parallel form. Figure 3.1 shows the PID controller structure.

Integral-Proportional Derivative controller (I-PD) is a modified form of PID controller. In it, the term known as integral is connected in path that is connected as forward and terms proportional and derivative are connected in path that is connected as reversed [28]. I-PD controller's integral terms is applied to the error signal. Figure 3.2 shows the I-PD controller structure.

3.3.1. PID Controller

The proposed design of PID controller is given as

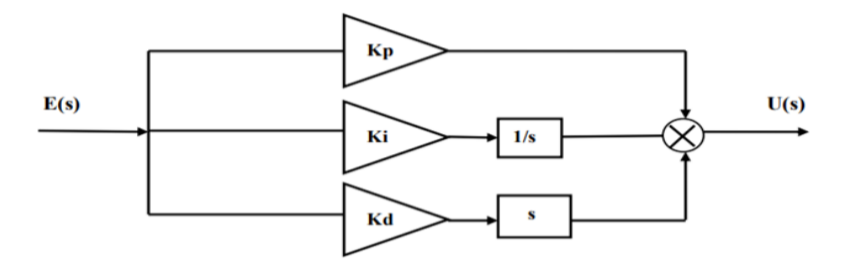


Figure 3.2: Structure of PID controller

Transfer function for PID controller from figure 3.1 and plant for Case-I and Case-II are shown in equation 3.37, 3.38 and 3.39.

$$Gc(s) = Kp + \frac{Ki}{s} + Kds$$
 (3.37)

$$G_{P1} = \frac{V_0(s)}{D(s)} = \frac{216000}{0.0006s^2 + s + 6000}$$
 (3.38)

$$G_{P2} = \frac{V_0(s)}{D(s)} = \frac{1280}{8e - 8s^2 + 0.001s + 8}$$
 (3.39)

Using equation 3.37 and 3.38, control structure for PID controller with transfer function for Case-I has been shown in Figure 3.3.

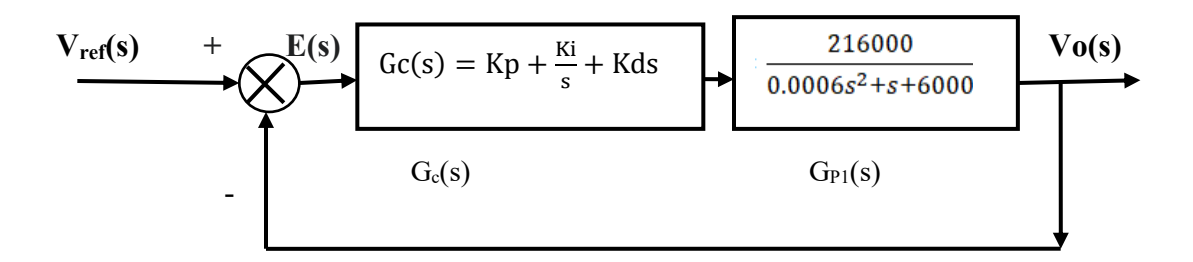


Figure 3.3: Control structure of PID controller for Case-I

As the equation for close loop unity feedback system with PID controller is [29]

$$\frac{V_0(s)}{V_{ref}(s)} = \frac{Gc(s)Gp1(s)}{1+Gc(s)Gp1(s)}$$
(3.40)

Putting values of $G_C(s)$ and $G_{P1}(s)$ from equation 3.37 and 3.38 in equation 3.40

$$\frac{V_0(s)}{V_{ref}(s)} = \frac{216000(Kps + Ki + Kds^2)}{0.0006s^3 + (1 + 216000Kd)s^2 + (6000 + 216000Kp)s + 216000Ki}$$
(3.41)

Using equation 3.37 and 3.39, control structure for PID controller with transfer function for Case-II has been shown in Figure 3.2.

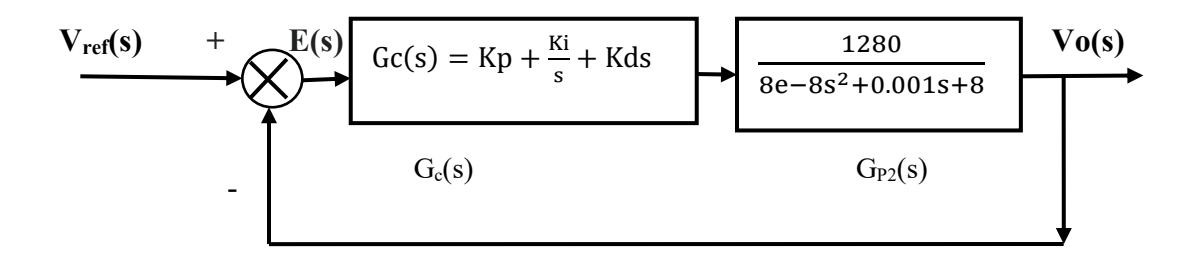


Figure 3.4: Control structure of PID controller for Case-II

As the equation for close loop unity feedback system with PID controller is [29]

$$\frac{Vo(s)}{V_{ref}(s)} = \frac{Gc(s)Gp2(s)}{1+Gc(s)Gp2(s)}$$
(3.42)

Putting values of $G_C(s)$ and $G_{P2}(s)$ from equation 3.37 and 3.39 in equation 3.42

$$\frac{V_0(s)}{V_{ref}(s)} = \frac{1280(Kps + Ki + Kds^2)}{8e - 8s^3 + (0.001 + 1280Kd)s^2 + (8 + 1280Kp)s + 1280Ki}$$
(3.43)

3.3.2. I-PD Controller

In Figure 3.5, I-PD controller structure is show.

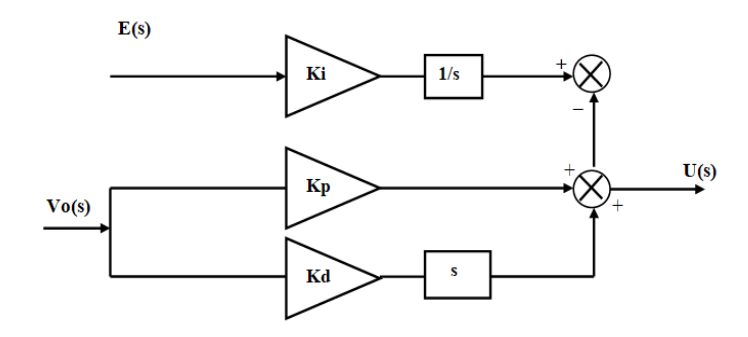


Figure 3.5: I-PD controller structure

Transfer function for I-PD controller and plant for Case-I and Case-II are shown in equation 3.44, 3.45 and 3.46.

$$Gc(s) = \frac{Ki}{s} - (Kp + Kds)$$
 (3.44)

$$G_{P1} = \frac{V_0(s)}{D(s)} = \frac{216000}{0.0006s^2 + s + 6000}$$
 (3.45)

$$G_{P2} = \frac{V_0(s)}{D(s)} = \frac{1280}{8e - 8s^2 + 0.001s + 8}$$
 (3.46)

Using equation 3.44 and 3.45, control structure for I-PD controller with transfer function for Case-I has been shown in Figure 3.6.

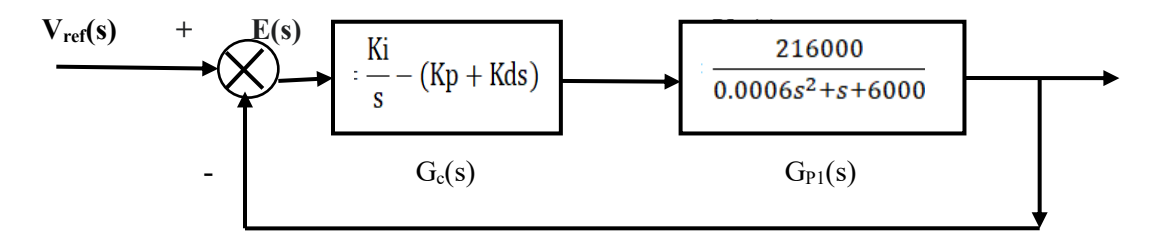


Figure 3.6: Control structure of I-PD controller for Case-I

As the equation for close loop unity feedback system with I-PD controller is [30]

$$\frac{V_0(s)}{V_{ref}(s)} = \frac{Gi(s)Gp1(s)}{1 + Gp1(s)(Gi(s) + GpD(s))}$$
(3.47)

Put value of $G_i(s)$ and $G_{P1}(s)$ from equation 3.44 and 3.45 in equation 3.47

$$\frac{V_0(s)}{V_{ref}(s)} = \frac{216000 \text{Ki}}{6e - 4s^3 + (1 + 216000 \text{Kd})s^2 + (6000 + 216000 \text{Kp})s + 2160000 \text{Ki}}$$
(3.48)

Using equation 3.44 and 3.46, control structure for I-PD controller with transfer function for Case-II has been shown in Figure 3.7.

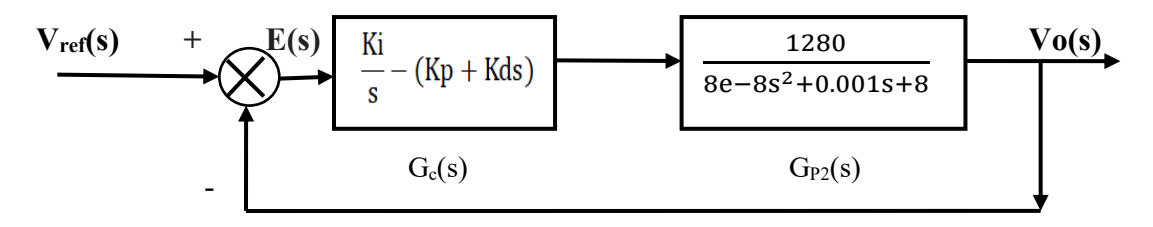


Figure 3.7: Control structure of I-PD controller for Case-II

$$\frac{V_{o}(s)}{V_{ref}(s)} = \frac{Gi(s)Gp2(s)}{1 + Gp2(s)(Gi(s) + G_{PD}(s))}$$
(3.49)

Put value of $G_i(s)$ and $G_{P2}(s)$ from equation 3.44 and 3.46 in equation 3.49

$$\frac{V_o(s)}{V_{ref}(s)} = \frac{1280Ki}{8e - 8s^3 + (0.001 + 1280Kd)s^2 + (8 + 1280Kp)s + 1280Ki}$$
(3.50)

3.4. Evolutionary Computing Techniques

There are several methods that are used by the researchers to find the optimum perimeters for controllers like K_p , K_i , K_d . Researchers have used methods like Ziegler Nicholas (ZI), and Cohencoon method for tuning of controller [31]. A desired objective function is selected and metaheuristic algorithms are applied to get the optimum solution. In this research, GWO, JSO and FDO optimization techniques has been used to find the best values of gains of proposed controller. Brief description of proposed optimization techniques along with their flow charts are given in below sections.

3.4.1. Grey Wolf Optimization Algorithm (GWO)

This algorithm is swarm intelligence based and proposed by Seyedali Mirjalili, Seyed Mohammad Mirjahlili and Andrew Lewis. In this algorithm, hierarchy and mechanism of hunting of wolfs society is used. Their whole society is usually made upof 5-12 wolfs. The pack of world is socially divided into four type of wolfs depending on the dominance of these wolfs in the society. Alpha wolfs are consider as the leader of the group and they are responsible for taking decisions for whole group. Alphas are not the strongest wolf of the group but have leadership qualities to handle the whole pack. Betas are considered the subordinates of alphas and help the alphas in decision making. Delta are considered as caretakers, and elder wolfs while omega are consider as the lowest in the group. The hunting mechanism of grey wolf is basically divided into 3 stages: prey searching, prey encircling and

prey attacking. In mathematical model of Grey wolf all these stages along with social hierarchy is used.

In order to update the position of each wolf, we need to define two position vectors A and C

$$A = 2\alpha r_1 \alpha \tag{3.51}$$

And
$$C = 2. r_2 \tag{3.52}$$

Where r_1, r_2 vectors are random and their values lie in [0, 1]. Variable α value decrease randomly from 2-0. To find updated location of each grey wolf, average of three best positions will be taken as shown below.

$$X(t+1) = \frac{X_1 + X_2 + X_3}{3} \tag{3.53}$$

Where

$$X_1 = X_{\alpha} - A_1 \cdot (D_{\alpha}), X_2 = X_{\beta} - A_2 \cdot (D_{\beta}), X_3 = X_{\gamma} - A_3 \cdot (D_{\gamma})$$
 (3.54)

$$D_{\alpha} = |C_1 X_{\alpha} - X|, D_{\beta} = |C_2 X_{\beta} - X|, D_{\gamma} = |C_3 X_{\gamma} - X|$$
 (3.55)

Figure 3.8 shows the brief overview of GWO.

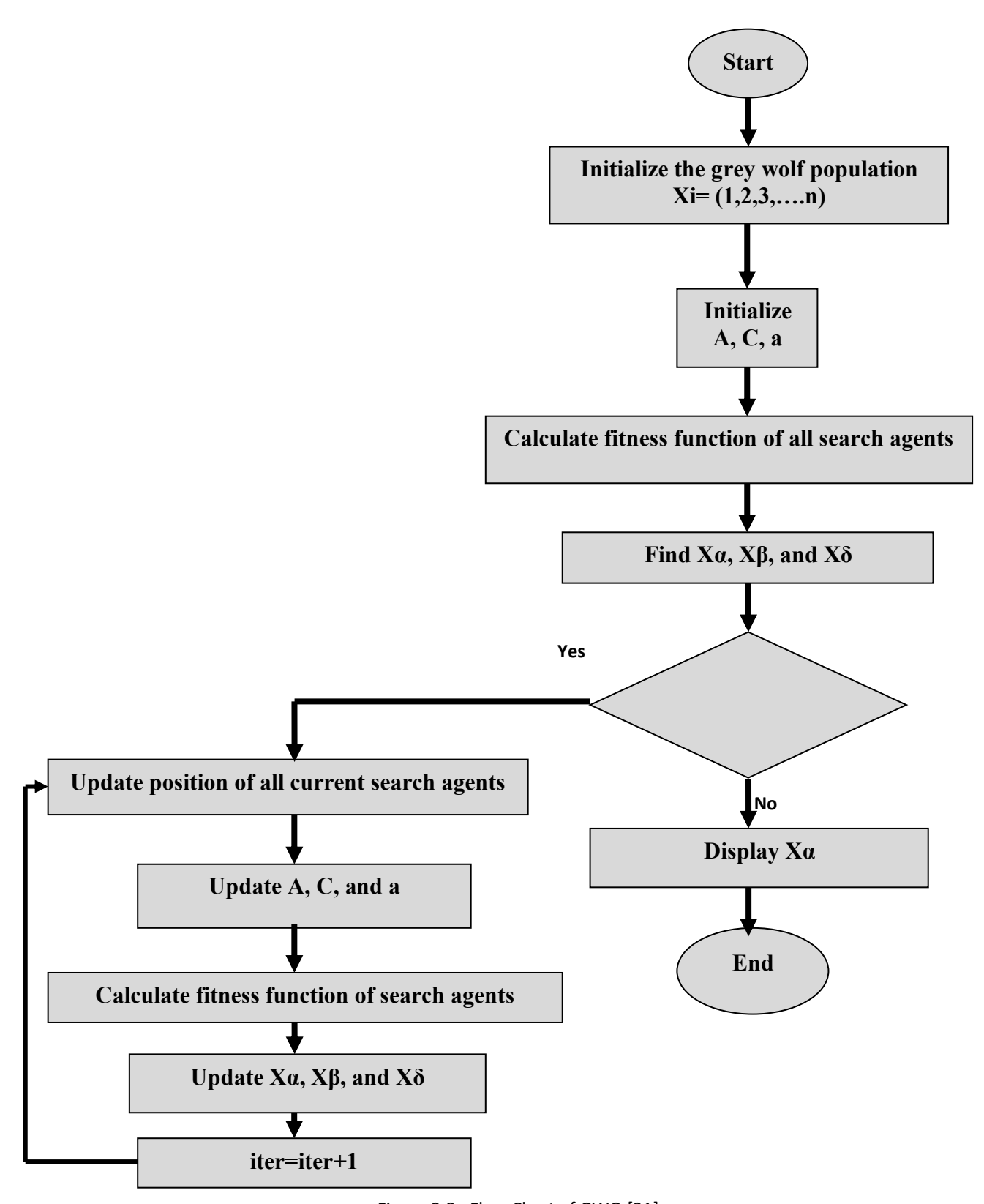


Figure 3.8: Flow Chart of GWO [31].

3.4.2. Jellyfish Search Optimization Algorithm (JSO)

The Jellyfish Search Optimization Algorithm is a newly proposed metaheuristic searching algorithm that is based on the movement of jellyfish inside the swarm and movement of jellyfish under ocean current. Ocean current contains large amount of nutrients and jellyfish usually follows ocean currents. When huge number of jellyfish follows ocean current in search of food, swarm is formed. After formation of swarm, some jellyfish feed themselves through filter feeding and some used tentacles to sting their prey. There is a time control mechanism that usually controls whether jellyfish will move in swarm or it will follows ocean current. The algorithm starts with defining objective function, setting search space, setting population size and number of iterations. Then the population of jellyfish is initialized by using chaotic map. Based on value of objective function, jellyfish at best location is determined and it is (X^*) . After that time control mechanism starts that basically decide the movement of jellyfish either jellyfish follows ocean current or it will move within the swarm. Equation for time control mechanism is given below.

$$c(t) = \left| \left(1 - \frac{t}{\text{Max}_{\text{iter}}} \right) x(2x \text{rand}(0,1) - 1 \right|$$
 (3.56)

After finding the value of time control mechanism, it is decided that whether new or updated position of jellyfish is calculated using ocean current equation or type A and type B motion equation. The new position of jellyfish when it follows ocean current can be determined by equations given below.

trent =
$$X^* - \beta \times rand(0,1) \times \mu$$
 (3.57)

$$X_i(t+1) = X_i(t) + rand(0,1) \times X^* - \beta \times rand(0,1) \times \mu$$
 (3.58)

The position of jellyfish can be calculated when type A movement occur within swarm by using equations given below.

$$X_i\left(t+1\right) = X_i(t) + \gamma \times rand(0,1) \times X^* - \beta \times rand(0,1) \times (U_b - L_b) \tag{3.59}$$

The position of jellyfish can be calculated when type B movement occurs within swarm by using equations given below.

Direction =
$$\begin{cases} X_j(t) - X_i(t) & \text{if } f(X_i) \ge f(X_j) \\ X_i(t) - X_j(t) & \text{if } f(X_i) < f(X_j) \end{cases}$$
 (3.60)

$$step = rand(0,1) \times Direction \tag{3.61}$$

$$X_{i}(t+1) = X_{i}(t) + \text{step}$$
 (3.62)

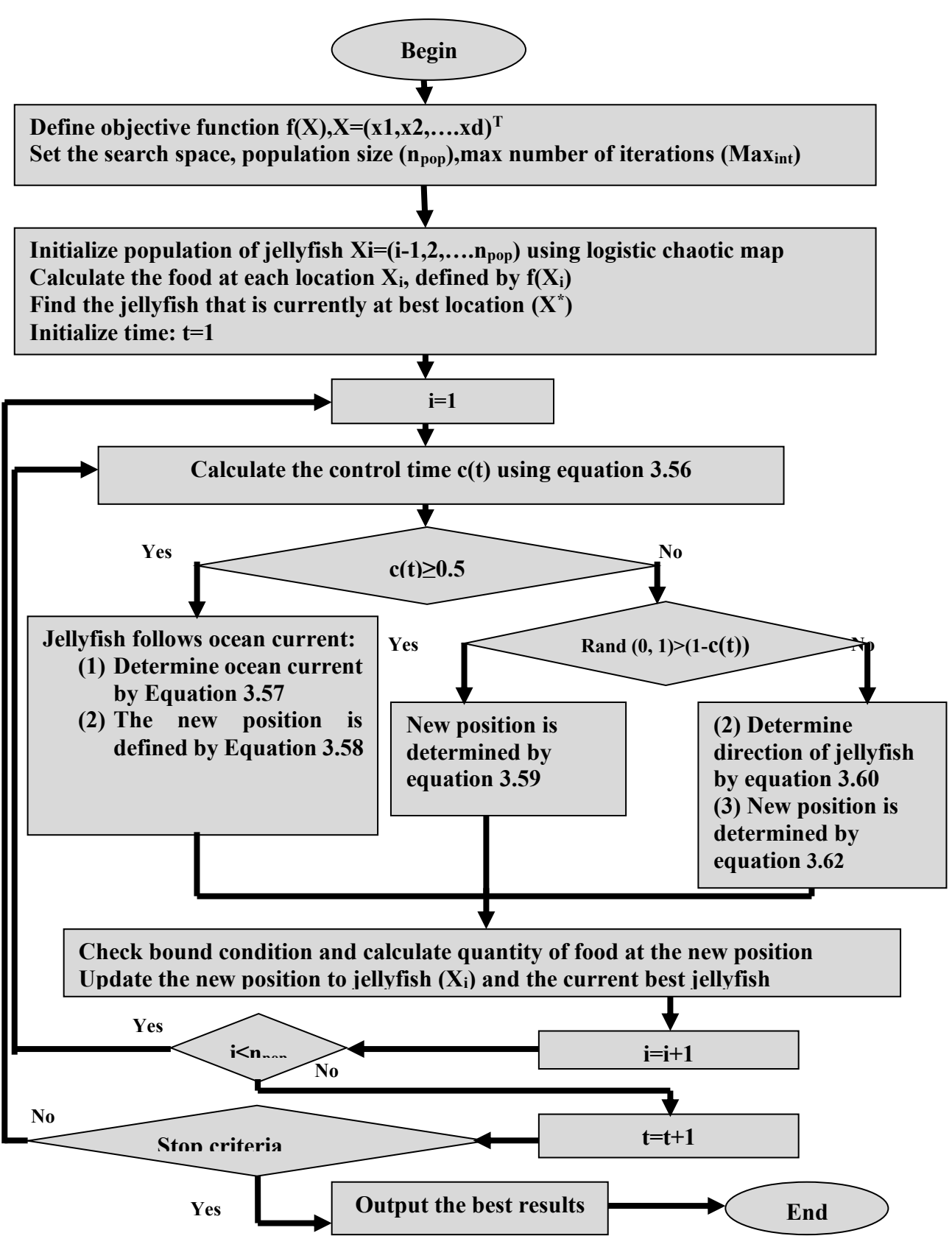


Figure 3.9: Flow chart of JSO [32].

3.4.3. Fitness dependent Optimization Algorithm (FDO)

Fitness dependent optimization algorithm is swarm intelligence based algorithm. It is designed on reproductive mechanism of bees swarm. In bee colony, there is a queen bee, scout bees and worker bees. Duty of queen bee is to lay egg and increase the number of bees in bee colony. Duty of worker bee is to build new cells of hive to accommodate new bees. Scout bees protect the hive and area around the hive and also search new hives when needed. Near spring season, queen bee along with some of worker and scout bees leave the old hive and move toward new hive to lay eggs. The queen bee and worker bee settle on a temporary hive that is 20-30 meters away from the old hive. 20-30 scout bees move in search of new hive for queen. Scout bees move randomly in search of hive and try to find the best hive for the queen. Whenever the scout bee finds the suitable hive, they communicate with each other through bee dance to tell other scout bees about that particular hive. Scout bees continue searching for new hive if they find a new hive that is much better than the previous one otherwise they will go back to that previous best hive and again start searching around that hive. Scout bees continue searching for new hive until 80% of the scout bees agree on particular hive suitability then the queen bees and worker bees follow scout bees and move to that hive. This searching mechanism of new hive by honey bees is mathematically modeled in fitness dependent optimization algorithm for searching optimal solution. Before going into detail of flow chart of FDO, we will consider the mathematical model of FDO.

If X is scout bee and i is its current position, then the next best position can be finding out by using equation given below. The scout bee adds factor P which is pace to find the next best position [36].

$$X_{i,t+1} = X_{i,t} + pace$$
 (3.63)

The equation for finding fw is given below.

$$fw = \left| \frac{\mathbf{x}_{i,t,f}^* \text{fitness}}{\mathbf{x}_{i,t,f} \text{fitness}} \right| - wf \tag{3.64}$$

Where $x_{i,t}^*$ fitness and $x_{i,t}$, fitness shows fitness functions of best scout and normal scout. The factor wf shows the weight factor. The value of wf lies between [0,1]. The factor wf= 1 shows high convergence rate while wf= 0 shows does not affect above equation. The fw value is 1 when $x_{i,t,f}^*$ fitness equals $tox_{i,t}$, fitness. fw is 0 when $x_{i,t}^*$ fitness = 0. To prevent $x_{i,t}$, fitness = 0. Following conditions should be fulfilled.

$$\begin{cases} fw = 1 \text{ or } fw = 0 \text{ or } x_{i,t} \text{ fitness} = 0, pace = x_{i,t} * r \\ fw > 0 \text{ and } fw < 1 \end{cases} \begin{cases} r < 0, pace = \left(x_{i,t} - x_{i,t,f}^*\right) * fw * -1 \\ r > 0, pace = \left(x_{i,t} - x_{i,t,f}^*\right) * fw \end{cases} \tag{3.65}$$

Value of r range between [-1,1]. Block diagram for fitness dependent optimizer is shown below.

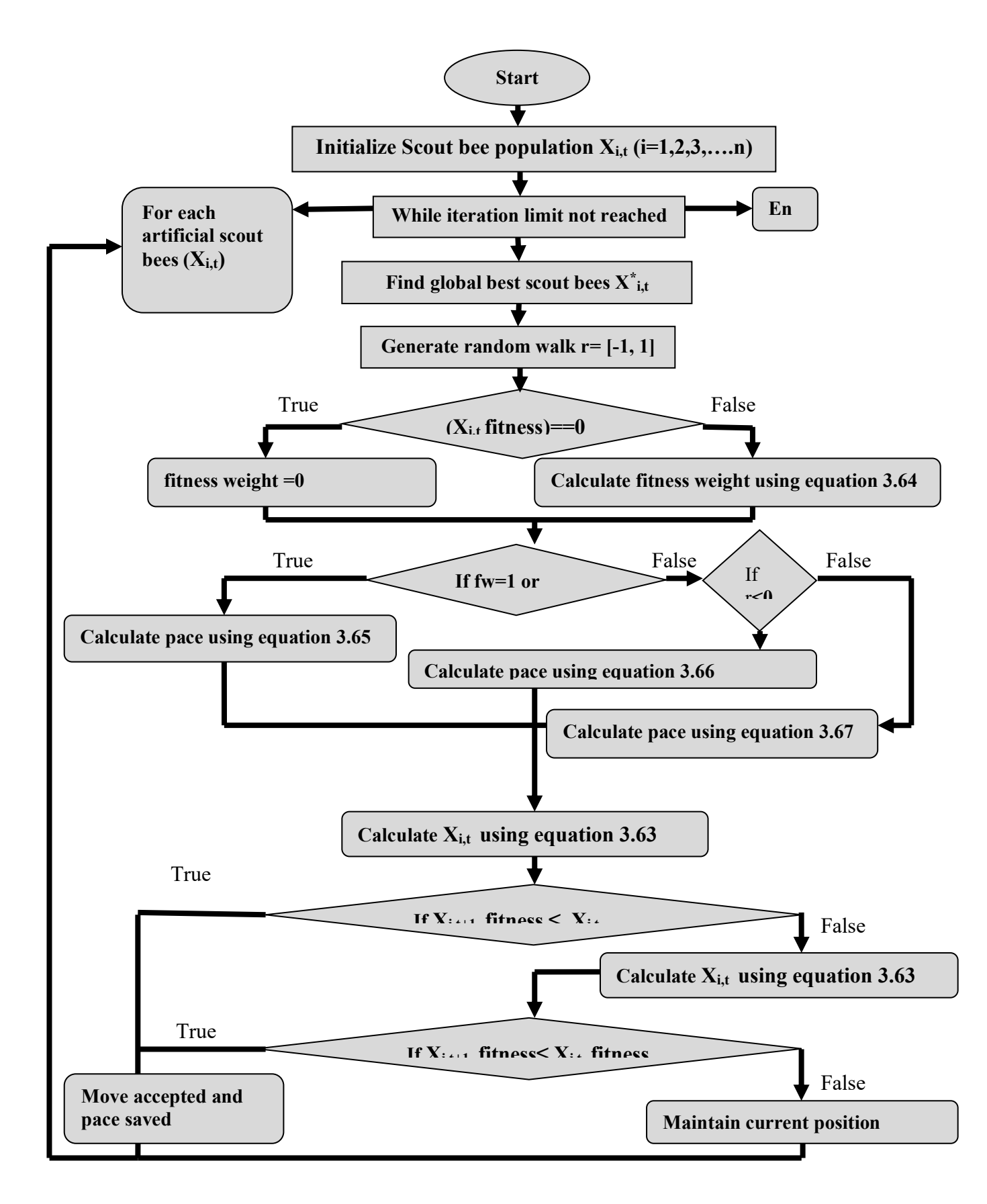


Figure 3.10: Flow chart of FDO [33].

Chapter 4 Formulation of objective function and performance indices 4.1. Objective function

Evolutionary computing techniques are used to find the controllers parameters values at which controller gives optimal response. Fitness function for proposed controller has been derived mathematically and this fitness function is used to find the fitness of solution generated from a particular optimization technique. The solution with best fitness value is considered as the best solution [34]. In this thesis, IAE, ISE, ITAE and ITSE have been considered as fitness functions and their relation has been derived mathematically for proposed controller for two cases of DC-DC buck converter.

4.2. Derivation of Error for PID and I-PD controller

As discussed in above sections, IAE, ISE, ITAE and ITSE are used as fitness function in this thesis. This chapter will deal with the derivation of objective function for PID and I-PD for both cases.

4.3. Case-I

4.3.1. Derivation of Error for PID controller

For case-I, when PID is connected with first transfer function derived and shown in equation 3.35 with unity feedback the block diagram will become as given below in figure 4.1.

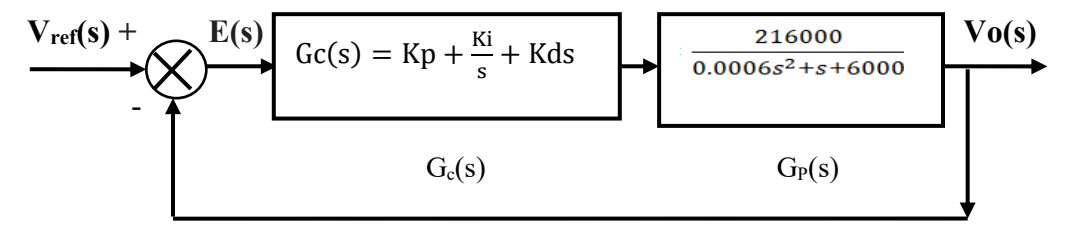


Figure 4.1: Control structure of PID control for Case-I

From Figure 4.1, E(s) is defined as difference between $V_{ref}(s)$ and $V_o(s)$ and it can be written

as shown in equation 4.1.

$$E(s) = V_{ref}(s) - V_{o}(s)$$
 (4.1)

$$V_{\text{ref}}(s) = \frac{1}{s} \tag{4.2}$$

From equation 3.41,

$$\frac{V_o(s)}{V_{ref}(s)} = \frac{216000(Kps + Ki + Kds^2)}{0.0006s^3 + (1 + 216000Kd)s^2 + (6000 + 216000Kp)s + 216000Ki}$$
(4.3)

Putting equation 4.2 and 4.3 in equation 4.1

$$E(s) = \left[\frac{0.0006s^2 + s + 6000}{0.0006s^3 + (1 + 216000Kd)s^2 + (6000 + 216000Kp)s + 216000Ki} \right]$$
(4.4)

Detail calculations of E(s) and error equation e (t) is shown in Appendix A.

4.3.2. Derivation of Error for I-PD controller

For case-I, when I-PD is connected with first transfer function derived and shown in equation 3.35 with unity feedback the block diagram will become as given below in figure 4.2.

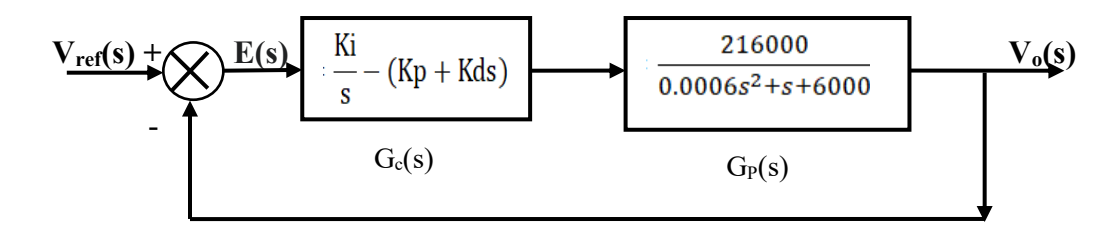


Figure 4.2: Control structure of I-PD control for Case-I

From Figure 4.2, E(s) is defined as difference between $V_{ref}(s)$ and $V_o(s)$ and it can be written as shown in equation 4.5.

$$E(s) = V_{ref}(s) - V_o(s)$$

$$(4.5)$$

$$V_{\text{ref}}(s) = \frac{1}{s} \tag{4.6}$$

From equation 3.48

$$\frac{V_o(s)}{V_{ref}(s)} = \frac{216000 \text{Ki}}{0.0006 \text{s}^3 + (1 + 216000 \text{Kd}) \text{s}^2 + (6000 + 216000 \text{Kp}) \text{s} + 216000 \text{Ki}}$$
(4.7)

Putting equation 4.6 and 4.7 in equation 4.5

$$E(s) = \left[\frac{0.0006s^2 + (1 + 216000Kd)s + (6000 + 216000Kp)}{0.0006s^3 + (1 + 216000Kd)s^2 + (6000 + 216000Kp)s + 216000Ki} \right]$$
(4.8)

Detail calculations of E(s) and error equation e(t) is shown in Appendix B.

4.4. Case-II

4.4.1. Derivation of Error for PID controller

For case-II, when PID is connected with second transfer function derived and shown in equation 3.36 with unity feedback the block diagram will become as given below in figure 4.3.

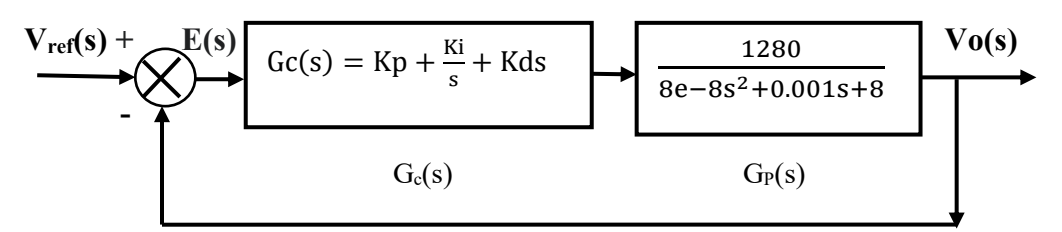


Figure 4.3: Control structure of PID control for Case-II

From Figure 4.3, E(s) is defined as difference between $V_{ref}(s)$ and $V_o(s)$ and it can be written as shown in equation 4.9.

$$E(s) = V_{ref}(s) - V_{o}(s)$$
 (4.9)

$$V_{\text{ref}}(s) = \frac{1}{s}$$
 (4.10)

From equation 3.43,

$$\frac{V_o(s)}{V_{ref}(s)} = \frac{1280(Kps + Ki + Kds^2)}{8e - 8s^3 + (0.001 + 1280Kd)s^2 + (8 + 1280Kp)s + 1280Ki}$$
(4.11)

Putting equation 4.10 and 4.11 in equation 4.9,

$$E(s) = \left[\frac{8e - 8s^2 + 0.0001s + 8}{8e - 8s^3 + (0.001 + 1280\text{Kd})s^2 + (1280 + 8\text{Kp})s + 1280\text{Ki}} \right] (4.12)$$

Detail calculations of E(s) and error equation e(t) is shown in Appendix C.

4.4.2. Derivation of Error for I-PD controller

For case-II, when I-PD is connected with first transfer function derived and shown in equation 3.36 with unity feedback the block diagram will become as given below in figure 4.4.

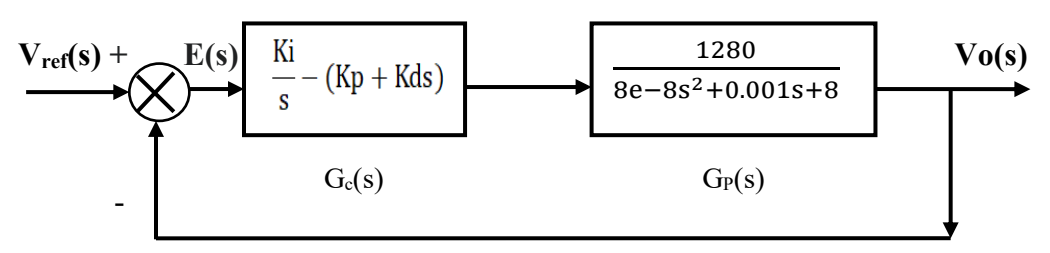


Figure 4.4: Control structure of I-PD control for Case-II

From Figure 4.4, E(s) is defined as difference between $V_{ref}(s)$ and $V_o(s)$ and it can be written as shown in equation 4.13.

$$E(s) = V_{ref}(s) - V_{o}(s)$$
 (4.13)

$$V_{\text{ref}}(s) = \frac{1}{s} \tag{4.14}$$

From equation 3.50,

$$\frac{V_{o}(s)}{V_{ref}(s)} = \frac{1280 \text{Ki}}{8e - 10s^{3} + (0.001 + 1280 \text{Kd})s^{2} + (1280 + 8 \text{Kp})s + 1280 \text{Ki}}$$
(4.15)

Putting equation 4.14 and 4.15 in equation 4.13

$$E(s) = \left[\frac{8e - 10s^2 + (0.001 + 1280\text{Kd})s + (1280 + 8\text{Kp})}{8e - 8s^3 + (0.001 + 1280\text{Kd})s^2 + (1280 + 8\text{Kp})s + 1280\text{Ki}} \right]$$
(4.16)

Detail calculations of E(s) and error equation e(t) is shown in Appendix D.

4.5. Performance Indices

Optimum response of system is related to minimum value of time domain performance

indices. In this thesis GWO, JSO and FDO has been used to get the minimum value of four performance indices that are IAE, ISE, ITAE and ITSE. At minimum value of these indices, optimum values of controllers exist.

4.5.1. Integral of absolute value of error (IAE)

IAE is defined as total error which is minimized over time as given in equation 4.17.

$$IAE = \int_0^T |e(t)| dt \tag{4.17}$$

In IAE all errors are treated equally whether positive or negative. As all errors are treated equally so response of system shows balance speed and time. IAE is slightly better than ISE as it shows critically damped response.

4.5.2. Integral of square error (ISE)

ISE is defined as square of error minimized over time as given in equation 4.18.

$$ISE = \int_0^T e^2(t)dt \tag{4.18}$$

Due to square term present in the above section, large errors are penalized heavily. ISE encourage quick correction and response is under damped.

4.5.3. Integral of time multiplied by absolute value of error (ITAE)

The error criteria in which error with increasing weight over time is minimized is known as ITAE as given in equation 4.19. Similar to IAE, response of ITAE is also critically damped with fast settling time and reduced steady state error.

$$ITAE = \int_0^T t|e(t)|dt \tag{4.19}$$

4.5.3. Integral of time multiplied by squared value of error (ITSE)

In ITSE, square of error with increase weight over time is minimized as shown in equation

4.20. In ITSE persistent and large errors are penalized. ITSE gives smooth and slower response. The response behavior is over damped.

$$ITSE = \int_0^T t|e^2(t)|dt \qquad (4.20)$$

Chapter 5 Implementation and Results

To investigate the proposed controllers step response for two different cases of selected system, system used is Dell Inc. with processor Intel(R) Core(TM) i5-8365U CPU @ 1.60 GHz, 1896 MHz, 4 Core(s), and 8 Logical Processor(s). For simulations, SIMULINK and MATLAB 2024b are used. The results obtained have been given in this chapter.

5.1. Step response of DC-DC buck converter for Case-I and Case-II without controller

In this research work, two different cases are considerered. Step response of these two cases are given in figure 5.1 and 5.2. In figure 5.1, for first case, the %OS is 42.3%, ts is 0.00443s and tr=0.000405.For Case-II %OS is 8.08 %, ts is 0.000598s and tr=0.000192.

For Case I:

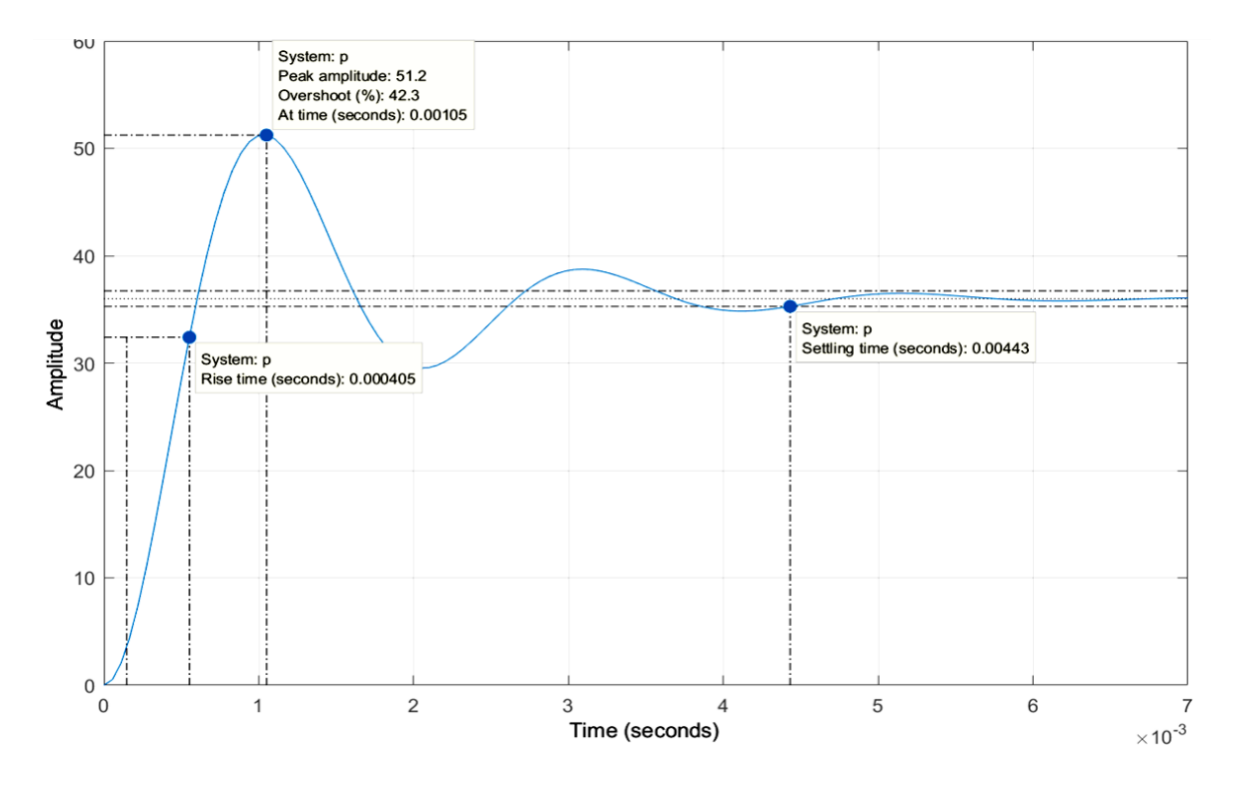


Figure 5.1: Step response for Case-I

For Case II

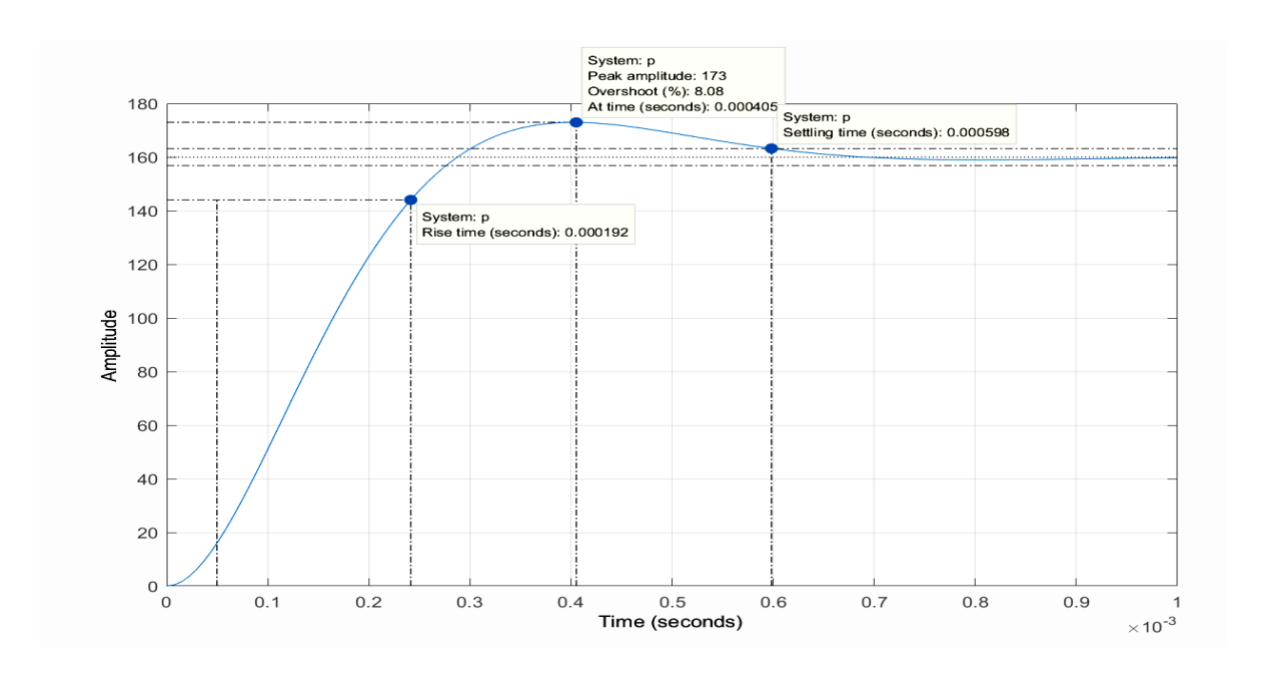


Figure 5.2: Step response for Case-II

5.2. Parameters Setting for GWO, JSO and FDO

In order to optimal tune the proposed controllers three tuning algorithms: GWO, JSO and FDO has been used. Settings for different parameters are given in Table 5.1.

Table 5.1: Parameters setting for GWO, JSO and FDO.

GWO	JSO	FDO
Population 30	Population 10	Population 20
Iterations 60	Iterations 40	Iterations 45
Lower Bound[1,0.01,0.001]	Lower Bound[1,0.01,0.001]	Lower Bound[1,0.01,0.001]
Upper Bound [50,10,10]	Upper Bound [50,10,10]	Upper Bound [50,10,10]
r ₁ ,r ₂ =[0,1] and a=[2,0]	γ=0.1,β=3	r=[-1,1]

5.3. Case-I

For case I, the transfer function from equation 3.35 is.

$$\frac{\text{Vo(s)}}{\text{D(s)}} = \frac{216000}{0.0006\text{s}^2 + \text{s} + 6000}$$

5.3.1. Control parameters of GWO-PID, JSO-PID, and FDO-PID controllers

The algorithms GWO, JSO, and FDO are executed for Case-I with PID controller. The optimal values of control parameters obtained for PID controller is given in the Table 5.2.

Table 5.2: Control parameters of GWO-PID, JSO-PID, and FDO-PID controllers

Tuning Algorithm	Error Criteria	PID		
		Кр	Ki	Kd
GWO	IAE	50	10	0.001
	ISE	50	10	0.001
	ITAE	1.0277	10	0.0019
	ITSE	50	10	0.0082
JSO	IAE	43.9499	4.71796	0.7891
	ISE	29.9442	6.57612	4.5955
	ITAE	33.2669	0.075788	0.0261
	ITSE	43.4107	0.389158	0.769
FDO	IAE	20.3432	5.6848	0.0010
	ISE	31.7422	0.1780	2.9178
	ITAE	47.2716	9.9363	1.3997
	ITSE	39.3231	2.2914	0.0010

5.3.2. Control parameters of GWO-I-PD, JSO-I-PD, and FDO-I-PD

controller

The algorithms GWO, JSO, and FDO are executed for Case-I of DC-DC converter with controller I-PD. The optimal values of control parameters obtained for I-PD controller is given in the Table 5.3.

Table 5.3: Control parameters of GWO-I-PD, JSO-I-PD, and FDO-I-PD controllers

Tuning Algorithm	Error Criteria	PID		
		Кр	Ki	Kd
GWO	IAE	10	1	0.0010
	ISE	10	1	0.0010
	ITAE	10	1	0.0011
	ITSE	10	1	0.0010
JSO	IAE	3.2386	2.2923	0.0032
	ISE	7.5346	3.8308	0.0045
	ITAE	8.5531	2.3904	0.0179
	ITSE	9.3412	5.6432	0.0549
FDO	IAE	22.3293	9.9999	0.0706
	ISE	18.335	10	0.0687
	ITAE	2.8229	6.6969	0.0343
	ITSE	5.4533	3.1995	0.0321

5.3.3. Step response of GWO-PID, JSO-PID, and FDO-PID controllers

In Figure 5.3, step response for PID controller for GWO, JSO and FDO is plotted. It can be seen that JSO-PID controller subjected to minimize ISE gives the fastest step response with

zero overshoot.

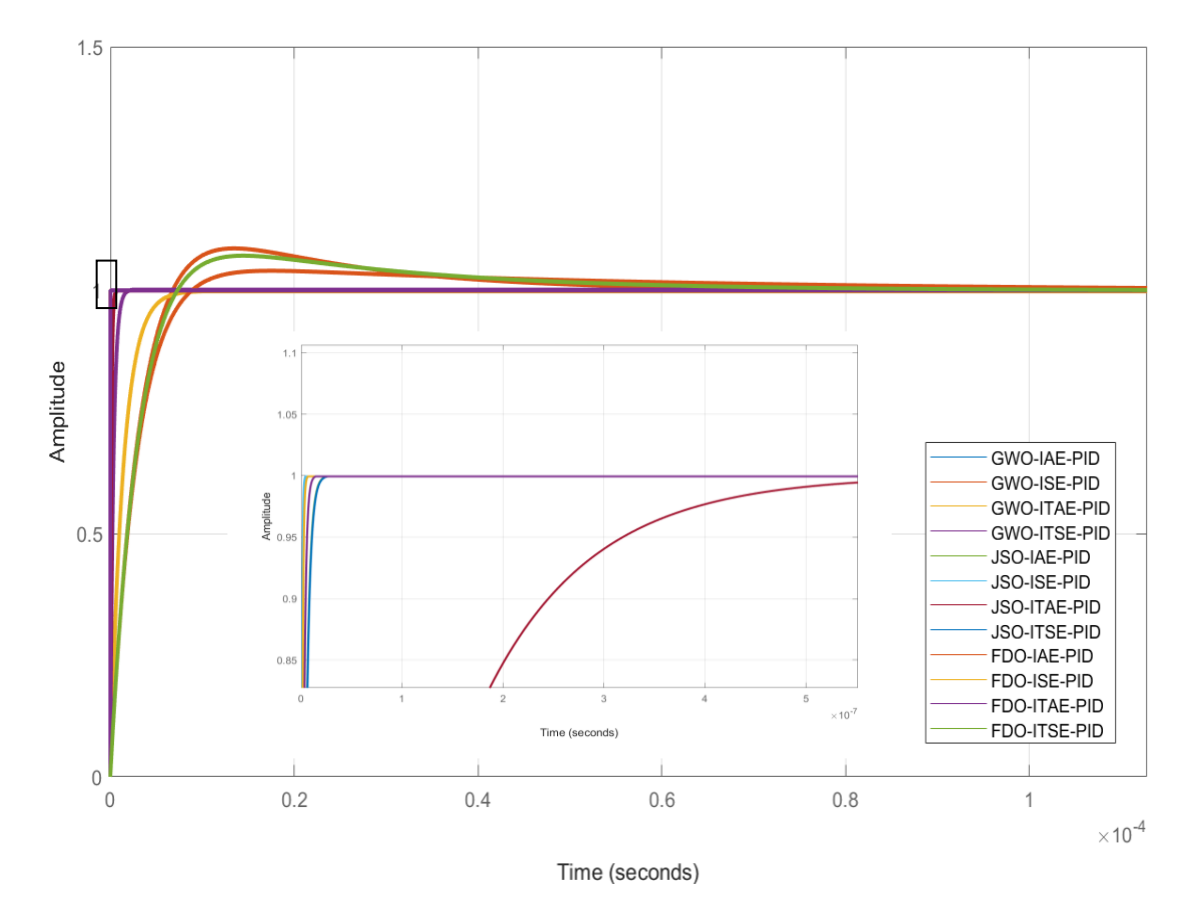


Figure 5.3: Step response of DC-DC Buck Converter System with GWO-PID, JSO-PID, and FDO-PID controllers for Case-I

5.3.4. Performance comparison of GWO-PID, JSO-PID, and FDO-PID controllers

Table 5.4 shows the JSO-PID controller subjected to minimize ISE gives the best performance in term of tr, ts, tp and %O.S. From the table 5.4, when JSO-PID controller subjected to minimize ISE is compared with GWO-PID controller subjected to minimize ISE, it is noted that tr, ts and tp has decreased by 99.97%, 99.99% and 99.996% respectively. Similarly when JSO-PID controller subjected to minimize ISE is compared with FDO-PID controller subjected to minimize ISE, it is noted that tr, ts and tp has decreased 57.5%, 36.50 and 57.50%

respectively.

Table 5.4: Performance comparison of GWO-PID, JSO-PID, and FDO-PID controllers

Tuning	Error Criteria	PID				
Algorithm		tr(s)	ts(s)	tp(s)	%OS	
GWO	IAE	4.6605e-06	4.1196e-05	1.3417e-05	8.5652	
	ISE	4.6605e-06	4.1196e-05	1.3417e-05	8.5652	
	ITAE	3.1023e-06	5.6056e-06	1.0270e-05	0	
	ITSE	7.3546e-07	1.2940e-06	2.4655e-06	0.0793	
JSO	IAE	7.7331e-09	1.3771e-08	2.5773e-08	0	
	ISE	1.3280e-09	2.3647e-09	4.4259e-09	0	
	ITAE	2.3365e-07	4.1620e-07	7.7859e-07	0	
	ITSE	7.9282e-09	1.4118e-08	2.6422e-08	0	
FDO	IAE	5.3643e-06	5.0823e-05	1.7467e-05	3.9698	
	ISE	2.0916e-09	3.7244e-09	6.9708e-09	0	
	ITAE	4.3601e-09	7.7640e-09	1.4531e-08	0	
	ITSE	4.8749e-06	4.5589e-05	1.4529e-05	7.0692	

5.3.5. Step response of GWO-I-PD, JSO-I-PD, and FDO-I-PD controllers

Step response for I-PD controller tuned by three algorithms GWO, JSO and FDO is given in the Figure 5.4. From the figure 5.4, it is shown that FDO-I-PD controller subjected to minimize IAE controller gives the fastest step response with zero overshoot.

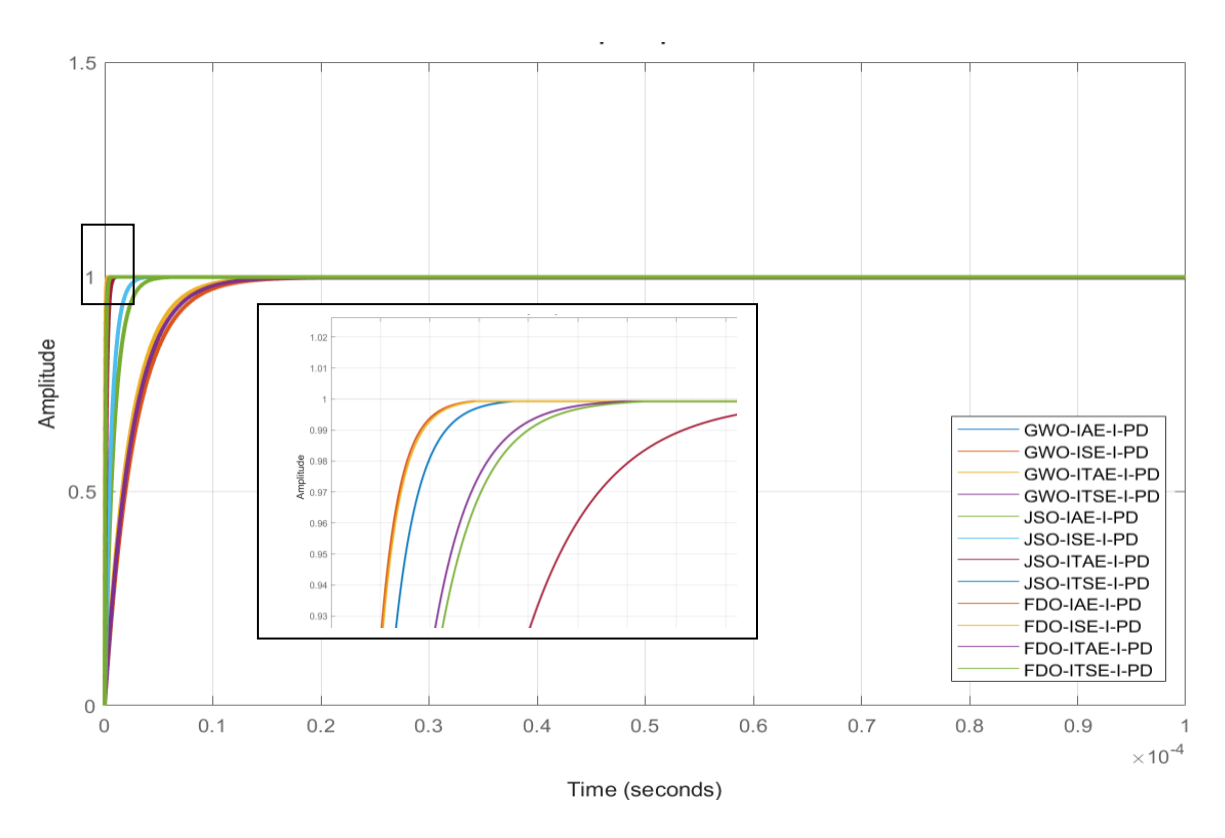


Figure 5.4: Step response of DC-DC Buck Converter System with GWO-I-PD, JSO-I-PD, and FDO-I-PD controllers for Case-I

5.3.6. Performance comparison of GWO-I-PD, JSO-I-PD, and FDO-I-PD controllers

Table 5.5 shows the FDO-I-PD subjected to minimize IAE controller gives the best performance in term of tr, ts, tp and %O.S. From the table 5.5, when FDO-I-PD controller subjected to minimize IAE is compared with GWO-I-PD controller subjected to minimize IAE, it is noted that tr, ts and tp has decreased by 98.46%, 98.48%, and 98.44% respectively. Similarly when FDO-I-PD controller subjected to minimize IAE is compared with JSO-I-PD controller subjected to minimize IAE, it is noted that tr,ts and tp has decreased 95.45%,95.48% and 99.54% respectively.

Table 5.5: Performance comparison of GWO-I-PD, JSO-I-PD, and FDO-I-PD controllers

Tuning	Error	I-PD				
Algorithm	Criteria	tr(s)	ts(s)	tp(s)	%OS	
GWO	IAE	5.6189e-06	1.0192e-05	1.8577e-05	0	
	ISE	6.1094e-06	1.1079e-05	2.0203e-05	0	
	ITAE	5.1717e-06	9.3805e-06	1.7098e-05	0	
	ITSE	5.6113e-06	1.0178e-05	1.8552e-05	0	
JSO	IAE	1.9037e-06	3.4071e-06	6.3298e-06	0	
	ISE	1.3309e-06	2.3702e-06	4.4352e-06	0	
	ITAE	3.3960e-07	6.0566e-07	1.1310e-06	0	
	ITSE	1.1101e-07	1.9780e-07	3.6987e-07	0	
FDO	IAE	8.6456e-08	1.5401e-07	2.8808e-07	0	
	ISE	8.8848e-08	1.5828e-07	2.9605e-07	0	
	ITAE	1.7800e-07	3.1729e-07	5.9291e-07	0	
	ITSE	1.9020e-07	3.3904e-07	6.3355e-07	0	

5.3.7. Performance comparison proposed controllers with reference papers

Table 5.6 shows the proposed controller's performance comparison with controllers given in reference paper. By comparing the transient characteristics of controllers proposed in this work with the controllers given in base paper, it is noted that JSO-PID controller subjected to minimize ISE has decreased tr, ts and tp by 99.53%, 99.52%, and 99.67%. Similarly when FDO-I-PD controller subjected to minimize IAE is compared with reference paper, it can be seen that tr,ts and tp has decreased by 69.67%, 71.63, and 78.95% respectively. However,

when JSO-PID subjected to minimize ISE is compared with FDO-I-PD subjected to minimize IAE, it is clear that JSO-PID subjected to minimize ISE gives better performance than FDO-I-PD subjected to minimize IAE in term of tr,ts, and tp.

Table 5.6: Performance comparison of proposed controllers with reference papers

Controller		Tr(s)	Ts(s)	Tp(s)	Мр
JSO-PID	ISE	1.3280e-09	2.3647e-09	4.4259e-09	0
FDO-I-PD	IAE	8.6456e-08	1.5401e-07	2.8808e-07	0
IHGS FOPI	D [3]	2.8510e- 07	5.0765e- 07	1.3686e-06	0
HGS FOPII) [3]	3.6454e- 07	6.4930e- 07	1.7496e-06	0
HHO PID [3]	4.3528e- 07	7.7523e- 07	2.089e- 06	0
LFD PIDA	[3]	5.7605e- 07	9.5433e- 07	1.5356e-06	0.0124
AEO PID [3	3]	6.4613e- 07	1.1454e- 06	2.0223e- 06	0

5.4. Case II

For case II, the transfer function from equation 3.36 is.

$$\frac{\text{Vo(s)}}{\text{D(s)}} = \frac{1280}{8e - 8 + 0.001s + 8}$$

5.4.1. Control parameters of GWO-PID, JSO-PID, and FDO-PID controllers

The algorithms GWO, JSO, and FDO are executed for Case-I with PID controller. The optimal values of control parameters obtained for PID controller is given in the Table 5.7.

Table 5.7: Control Parameters of GWO-PID, JSO-PID, and FDO-PID controllers

Tuning Algorithm	Error Criteria	PID		
		Кр	Ki	Kd
GWO	IAE	50	10	0.00100065
	ISE	50	10	0.001
	ITAE	50	7.41596	0.00157004
	ITSE	50	10	0.00174855
JSO	IAE	20.9688	5.70096	2.90501
	ISE	45.2363	9.80329	7.75768
	ITAE	28.0111	6.19956	5.34716
	ITSE	49.7843	0.823448	0.00123125
FDO	IAE	15.5962	4.3589	1.8553
	ISE	41.7748	8.6439	0.0010
	ITAE	38.1076	1.8219	2.5928
	ITSE	39.1202	2.3796	2.6658

5.4.2. Control parameters of GWO-I-PD, JSO-I-PD, and FDO-I-PD controllers

Algorithms GWO, JSO, and FDO are executed for Case-II of DC-DC converter with controller I-PD. Optimal values of control parameters obtained for I-PD controller is given in the Table 5.8.

Table 5.8: Control Parameters of GWO-I-PD, JSO-I-PD, and FDO-I-PD controllers

Tuning Algorithm	Error Criteria		I-PD		
		Кр	Ki	Kd	
GWO	IAE	7.2401	3.7748	0.0021109	
	ISE	9.0595	4.6643	0.002514	
	ITAE	4.4045	3.0617	0.0036014	
	ITSE	9.8111	6.8459	0.0053658	
JSO	IAE	6.8237	6.4792	0.0047549	
	ISE	4.1057	3.2987	0.0025303	
	ITAE	9.1544	6.6491	0.0055905	
	ITSE	9.655	8.585	0.0055232	
FDO	IAE	9.9784	12.3092	0.0057	
	ISE	9.9417	11.6374	0.0059	
	ITAE	10.0000	17.3492	0.0066	
	ITSE	10.0000	19.2739	1.0000e-	
				03	

5.4.3. Step response of GWO-PID, JSO-PID, and FDO-PID controllers

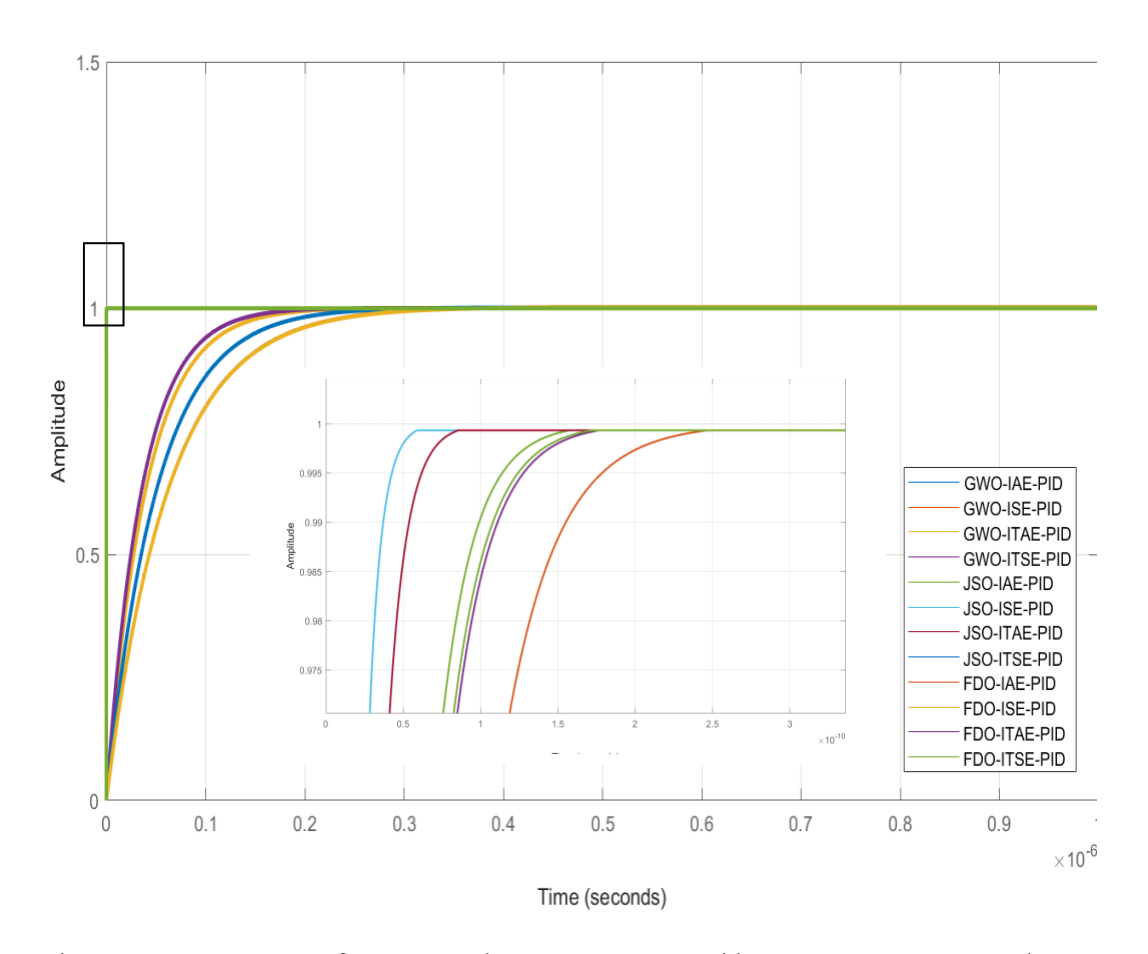


Figure 5.5: Step response of DC-DC Buck Converter System with GWO-PID, JSO-PID, and FDO-PID controllers for Case-II

In figure 5.5, step response for PID controller for Case-II tuned by GWO, JSO and FDO is plotted. It can be seen that JSO-PID controller subjected to minimize ISE gives the fastest step response with zero overshoot.

5.4.4. Performance comparison of GWO-PID, JSO-PID, and FDO-PID controllers

Table 5.9 shows that JSO-PID controller subjected to minimize ISE gives the best performance in term of tr, ts, tp and %O.S. For JSO-PID controller subjected to minimize ISE, overshoot has decreased to 0% as compared to GWO-PID and FDO-PID controllers subjected to minimize ISE From the table 5.5, when JSO-PID controller subjected to

minimize ISE is compared with GWO-PID controller subjected to minimize ISE, it is noted that tr, ts and tp has decreased by 99.9%, 99.98% and 99.98% respectively. Similarly when JSO-PID controller subjected to minimize ISE is compared with FDO-PID controller subjected to minimize ISE, it is noted that tr, ts and tp has decreased 99.98%, 99.986% and 99% respectively.

Table 5.9: Performance comparison GWO-PID, JSO-PID, and FDO-PID controllers

Tuning	Error Criteria	PID				
Algorithm		tr(s)	ts(s)	tp(s)	%OS	
GWO	IAE	1.3628e-07	2.3818e-07	4.5842e-07	0.1643	
	ISE	1.3636e-07	2.3832e-07	4.5872e-07	0.1646	
	ITAE	8.7260e-08	1.5438e-07	2.9171e-07	0.0103	
	ITSE	7.8396e-08	1.3893e-07	2.6188e-07	0	
JSO	IAE	4.7268e-11	8.4167e-11	1.5753e-10	0	
	ISE	1.7700e-11	3.1518e-11	5.8992e-11	0	
	ITAE	2.5680e-11	4.5726e-11	8.5585e-11	0	
	ITSE	1.1106e-07	1.9548e-07	3.7222e-07	0.0742	
FDO	IAE	7.4011e-11	1.3179e-10	2.4667e-10	0	
	ISE	1.3657e-07	2.3961e-07	4.5848e-07	0.1144	
	ITAE	5.2959e-11	9.4302e-11	1.7650e-10	0	
	ITSE	5.1509e-11	9.1719e-11	1.7167e-10	0	

5.4.5. Step response of GWO-I-PD, JSO-I-PD, and FDO-I-PD controllers

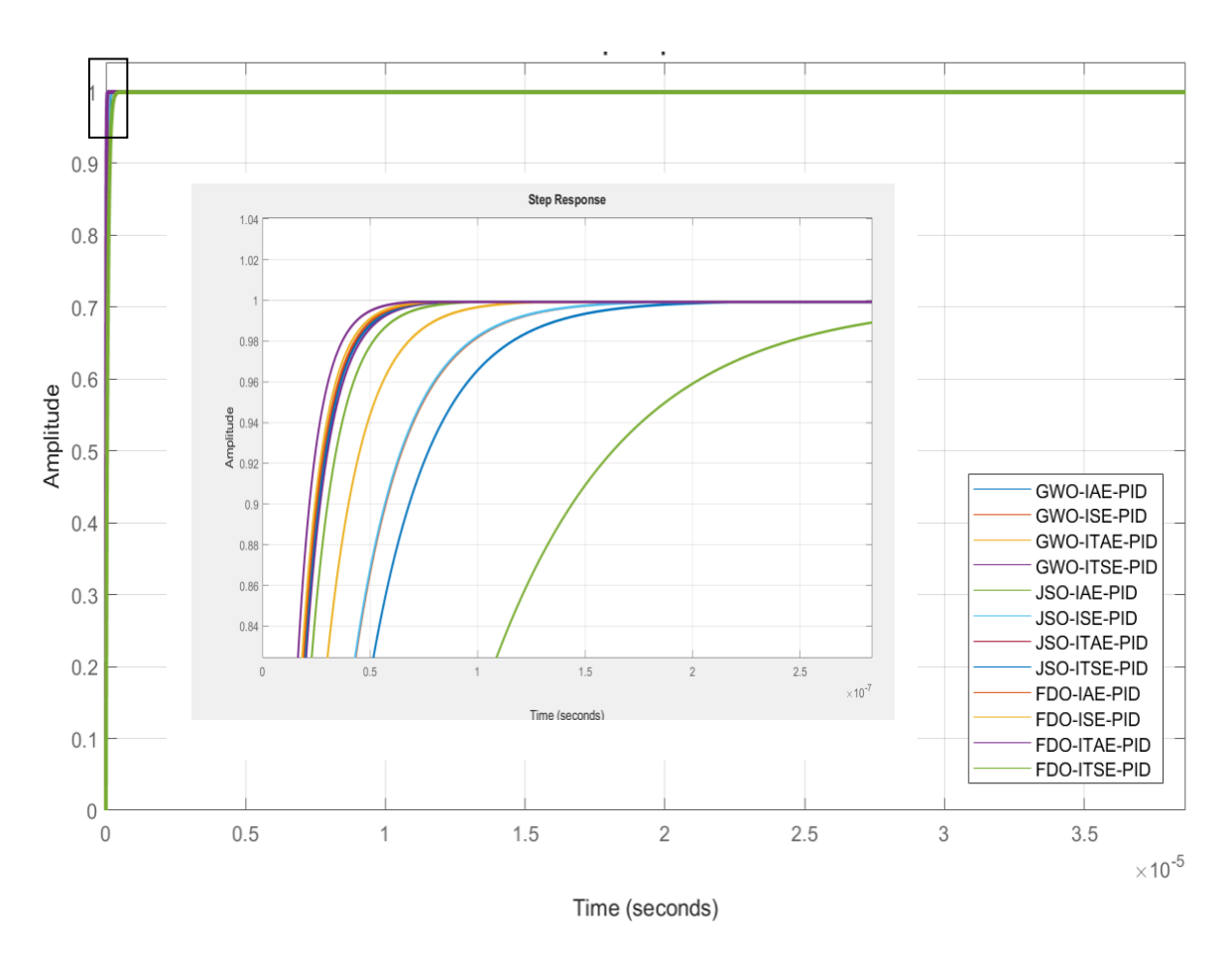


Figure 5.6: Step response of DC-DC Buck Converter System with GWO-I-PD, JSO-I-PD, and FDO based I-PD controller for Case-II

In figure 5.6, step response for I-PD controller for Case-II tuned by GWO, JSO and FDO is plotted. It can be seen that FDO-I-PD controller subjected to minimize ITAE gives the fastest step response with zero overshoot.

5.4.6. Performance comparison of GWO-I-PD, JSO-I-PD, and FDO-I-PD controllers

Table 5.10 demonstrate that FDO-I-PD controller subjected to minimize ITAE gives the best performance in term of tr, ts, tp and %O.S. Table 5.10 demonstrates that overshoot for controller; FDO-I-PD subjected to minimize ITAE is zero. When FDO-I-PD controller subjected to minimize ITAE is compared with GWO-I-PD controller subjected to minimize

ITAE, it is noted that tr, ts and tp has decreased by 45.44%, 45.49% and 45.42% respectively. Similarly when FDO-I-PD controller subjected to minimize ITAE is compared with JSO-I-PD controller subjected to minimize ITAE, it is noted that tr,ts and tp has decreased by 15.29, 15.31% and 15.12% respectively

Table 5.10: Performance comparison GWO-I-PD, JSO-I-PD, and FDO-I-PD controllers

Tuning	Error	I-PD				
Algorithm	Criteria	tr(s)	ts(s)	tp(s)	%OS	
GWO	IAE	6.5104e-08	1.1619e-07	2.1674e-07	0	
	ISE	5.4657e-08	9.7509e-08	1.8200e-07	0	
	ITAE	3.8151e-08	6.8047e-08	1.2705e-07	0	
	ITSE	2.5600e-08	4.5633e-08	8.5277e-08	0	
JSO	IAE	2.8891e-08	5.1509e-08	9.6232e-08	0	
	ISE	5.4313e-08	9.6936e-08	1.8081e-07	0	
	ITAE	2.4571e-08	4.3797e-08	8.1850e-08	0	
	ITSE	2.4871e-08	4.4331e-08	8.2847e-08	0	
FDO	IAE	2.4099e-08	4.2954e-08	8.0278e-08	0	
	ISE	2.3282e-08	4.1497e-08	7.7557e-08	0	
	ITAE	2.0812e-08	3.7091e-08	6.9332e-08	0	
	ITSE	1.3738e-07	2.4495e-07	4.5757e-07	0	

5.4.7. Performance comparison of proposed controllers with reference paper

When performance of proposed controllers tuned with GWO, JSO and FDO algorithms is

compared with DE-PID controller proposed in the reference paper, it can be seen that JSO-PID controller subjected to minimize ISE has reduced tr, and ts by 99.99%, and 99.99% respectively. FDO-PID subjected to minimize ITAE has reduced the tr and ts by 99.98% and 99.98% respectively. By comparing JSO-PID subjected to minimize ISE with FDO-I-PD subjected to minimize ITAE, it is clear that performance of JSO-PID subjected to minimize ISE is much better than FDO-I-PD subjected to minimize ITAE.

Table 5.11: Performance comparison of proposed controllers with reference papers

Controller		Tr(s)	Ts(s)	%OS
JSO-PID	ISE	1.7700e-11	3.1518e-11	0
FDO-I-PD	ITAE	2.0812e-08	3.7091e-08	0
DE PI	D [9]	1.57e-4	2.5e-4	0.0712

Chapter 6: Conclusion and Future Work

6.1. Conclusion

DC-DC buck converter is very important power electronic device use in several applications. Non linear behavior and fast dynamics of system introduces voltage fluctuations in the system so to avoid failure of device, voltage regulation is very important. Several controllers are used to regulate their output voltage. In this thesis we have selected two different transfer functions, for each transfer function, 2 controllers are designed to solve output voltage fluctuation issue and controllers parameters are optimized using three nature inspired heuristic algorithms that are GWO Algorithm, JSO Algorithm and FDO Algorithm.

In this study, when the performance of various controllers tuned with GWO, JSO, and FDO is compared with those from the base papers, including IHGS-FOPID, HGS-FOPID, HHO-PID, LFD-PIDA, and AEO-PID. By comparing the transient characteristics of proposed controllers with the controllers given in base paper, it has been found that JSO-PID controller subjected to minimize ISE outperforms other controllers by decreasing tr, ts and tp by 99.53%, 99.52%, and 99.67%.

For the second case, where the performance of GWO, JSO and FDO based PID and I-PD controllers were compared with DE PID, the JSO-PID controller subjected to minimize ISE has reduced tr, and ts by 99.99%, and 99.99% respectively and gives better results than other controllers.

These findings highlight the significant improvement in controller performance when tuned with JSO and FDO techniques, especially for the JSO-PID subjected to minimize ISE offers the most reliable and efficient control response.

6.2. Future Recommendation:

The research work in this study is largely based on the classified literature from the past two years as well as the latest methodologies, techniques and the best performing controllers that have already proved outstanding results in the past more or less numerous studies. These contemporary approaches have been ensured for system analysis and optimization in benefiting from contemporary tools of studies of systems and their optimization. Yet this research is comprehensive but it is worth to mention there is always room for improvement and innovation. This allows for further work to be done to overcome those current limitations, increase the system performance and define a more efficient way of controlling it.

- The detailed analysis on this study provides several future directions. The first
 recommendation is to adopt some other controllers such as PI-PD, TID, MRPID,
 PIDA, and PIDD2-PI which are inside the scope of the tuning and optimizing of the
 selected system. Exploring these controllers could provide valuable insights into the
 system's performance and optimization potential under various conditions.
- 2. The second recommendation is to further explore the unexplored metaheuristic optimization techniques in terms of the selection system. Overall, the Fox Optimization Algorithm, Snake Optimizer, White Shark Optimizer, Flying Fox Optimization Algorithm, Spider Wasp Optimization, and Termite Life Cycle Optimizer have not been fully tested for this particular system, but these particular systems present very promising opportunities of improving the optimization process itself. The researchers then applied these innovative techniques to help find new solutions that would further increase the efficiency and robustness of the system.

These directions have a great potential for future research which would be greatly valuable for the study of the control systems at this level.

References

- U. Rahat, A. Basit, and M. Salman, "Voltage control for DC-DC converters," Preprints, 2018.
- 2. H. Shayeghi, A. Rahnama, N. Takorabet, P. Thounthong, and N. Bizon, "Designing a multi-stage PD(1+PI) controller for DC–DC buck converter," Energy Reports, vol. 8, pp. 765–773, Dec. 2022, doi: https://doi.org/10.1016/j.egyr.2022.10.448.
- 3. Davut Izci and Serdar Ekinci, "A novel improved version of hunger games search algorithm for function optimization and efficient controller design of buck converter system," e-Prime, vol. 2, pp. 100039–100039, Jan. 2022, doi: https://doi.org/10.1016/j.prime.2022.100039.
- 4. H. Shayeghi, A. Rahnama, N. Takorabet, P. Thounthong, and N. Bizon, "Designing a multi-stage PD(1+PI) controller for DC–DC buck converter," Energy Reports, vol. 8, pp. 765–773, Dec. 2022, doi: https://doi.org/10.1016/j.egyr.2022.10.448.
- 5. B. Hekimoglu and S. Ekinci, "Optimally Designed PID Controller for a DC-DC Buck Converter via a Hybrid Whale Optimization Algorithm with Simulated Annealing," Electrica, vol. 20, no. 1, pp. 19–27, Feb. 2020, doi: https://doi.org/10.5152/electrica.2020.19034.
- 6. D. Izci, B. Hekimoğlu, and S. Ekinci, "A new artificial ecosystem-based optimization integrated with Nelder-Mead method for PID controller design of buck converter," Alexandria Engineering Journal, vol. 61, no. 3, pp. 2030–2044, Mar. 2022, doi: https://doi.org/10.1016/j.aej.2021.07.037.
- 7. L. K. Fong, M. S. Islam, and M. A. Ahmad, "Optimized PID Controller of DC-DC Buck Converter based on Archimedes Optimization Algorithm," International Journal of

- Robotics and Control Systems, vol. 3, no. 4, pp. 658–672, Sep. 2023, doi: https://doi.org/10.31763/ijrcs.v3i4.1113.
- 8. Norsyahidatul Farah Nanyan, Mohd Ashraf Ahmad, and Baran Hekimoğlu, "Optimal PID Controller for the DC-DC Buck Converter using the Improved Sine Cosine Algorithm," Results in Control and Optimization, vol. 14, pp. 100352–100352, Mar. 2024, doi: https://doi.org/10.1016/j.rico.2023.100352.
- Y. Zhao, Q. Qiu, and X. Zhao, "PID Parameter Tuning for Buck Controllers Based on an Improved Differential Evolution Algorithm," Journal of Physics: Conference Series, vol. 2029, no. 1, p. 012059, Sep. 2021, doi: https://doi.org/10.1088/1742-6596/2029/1/012059.
- 10. Asma Alfergani, Salma Elkawafi, T. M. Nour, Khawla Mohamed Elkezza, and Ashraf Kahlil, "Performance Evaluation of DC-DC Buck Converter with Voltage Control Loop Using Genetic Algorithm with Different Objective Functions," 2023 IEEE 3rd International Maghreb Meeting of the Conference on Sciences and Techniques of Automatic Control and Computer Engineering (MI-STA), pp. 135–140, May 2023, doi: https://doi.org/10.1109/MI-STA57575.2023.10169481.
- J. Zou and P. Xue, "Research on Control Strategy of Buck Converter Based on Particle Swarm Optimization Fuzzy PID," Journal of Physics: Conference Series, vol. 2395, no.
 p. 012044, Dec. 2022, doi: https://doi.org/10.1088/1742-6596/2395/1/012044.
- P. Warrier and P. Shah, "Optimal Fractional PID Controller for Buck Converter Using Cohort Intelligent Algorithm," Applied System Innovation, vol. 4, no. 3, p. 50, Aug. 2021, doi: https://doi.org/10.3390/asi4030050.

- I. Mohammed, "Design of Optimized PID Controller Based on ABC Algorithm for Buck," Journal of Engineering Science and Technology, vol. 16, no. 5, pp. 4040–4059, 2021, Accessed: Dec. 16, 2024. [Online]. Available: https://jestec.taylors.edu.my/Vol%2016%20Issue%205%20October%202021/16_5_29. pdf
- L. T. Rasheed, "Bat Algorithm Based an Adaptive PID Controller Design for Buck Converter Model," Journal of Engineering, vol. 26, no. 7, pp. 62–82, Jul. 2020, doi: https://doi.org/10.31026/j.eng.2020.07.05.
- S. M. Ghamari, H. G. Narm, and H. Mollaee, "Fractional-order fuzzy PID controller design on buck converter with antlion optimization algorithm," IET Control Theory & Applications, vol. 16, no. 3, pp. 340–352, Dec. 2021, doi: https://doi.org/10.1049/cth2.12230.
- M. A. Itaborahy et al., "Bio-Inspired Optimization Algorithms Applied to the GAPID Control of a Buck Converter," Energies, vol. 15, no. 18, pp. 6788–6788, Sep. 2022, doi: https://doi.org/10.3390/en15186788.
- 17. D. Bakria, M. Azzouzi, and D. Gozim, "Chaos Control and Stabilization of a PID Controlled Buck Converter Using the Spotted Hyena Optimizer," Engineering Technology & Applied Science Research, vol. 11, no. 6, pp. 7922–7926, Dec. 2021, doi: https://doi.org/10.48084/etasr.4585.
- 18. M. E. Çimen, Z. B. Garip, and A. F. Boz, "Chaotic flower pollination algorithm based optimal PID controller design for a buck converter," Analog Integrated Circuits and Signal Processing, vol. 107, no. 2, pp. 281–298, Jan. 2021, doi: https://doi.org/10.1007/s10470-020-01751-5.

- 19. Mirza Muntasir Nishat, F. Faisal, Anik Jawad Evan, M. Rahaman, Md. Sadman Sifat, and H. M. Fazle Rabbi, "Development of Genetic Algorithm (GA) Based Optimized PID Controller for Stability Analysis of DC-DC Buck Converter," Journal of Power and Energy Engineering, vol. 08, no. 09, pp. 8–19, Sep. 2020, doi: https://doi.org/10.4236/jpee.2020.89002.
- 20. A. Debnath, T. O. Olowu, S. Roy, I. Parvez, and Arif Sarwat, "Particle Swarm Optimization-based PID Controller Design for DC-DC Buck Converter," 2021 North American Power Symposium (NAPS), Nov. 2021, doi: https://doi.org/10.1109/naps52732.2021.9654737.
- 21. A. A. Chlaihawi, "Genetic algorithm error criteria as applied to PID controller DC-DC buck converter parameters: an investigation," IOP Conference Series: Materials Science and Engineering, vol. 671, p. 012032, Jan. 2020, doi: https://doi.org/10.1088/1757-899x/671/1/012032.
- 22. mohammad javad ghorbani, mahdi yosefi, Seyyed morteza ghamari, and Ebrahim Mahdavipoor, "Fractional-Order PID Controller Design on Buck Converter with Antlion Optimizer Algorithm," Authorea (Authorea), Nov. 2022, doi: https://doi.org/10.22541/au.166898280.03724131/v1.
- 23. A. Daraz, S. A. Malik, H. Mokhlis, I. U. Haq, G. F. Laghari, and N. N. Mansor, "Fitness Dependent Optimizer-Based Automatic Generation Control of Multi-Source Interconnected Power System With Non-Linearities," IEEE Access, vol. 8, pp. 100989–101003, 2020, doi: https://doi.org/10.1109/access.2020.2998127.
- 24. A. Daraz, S. A. Malik, I. U. Haq, K. B. Khan, G. F. Laghari, and F. Zafar, "Modified PID controller for automatic generation control of multi-source interconnected power

- system using fitness dependent optimizer algorithm," PLoS ONE, vol. 15, no. 11, p. e0242428, Nov. 2020, doi: https://doi.org/10.1371/journal.pone.0242428.
- 25. Tufan Dogruer, "Grey Wolf Optimizer-Based Optimal Controller Tuning Method for Unstable Cascade Processes with Time Delay," Symmetry, vol. 15, no. 1, pp. 54–54, Dec. 2022, doi: https://doi.org/10.3390/sym15010054.
- 26. B. Subedi, "Buck Converter: Basics, Working, Design & Application," How To Electronics, Sep. 16, 2022. https://how2electronics.com/buck-converterbasicsworking-design-application/#:~:text=Buck%20Converter%20is%20a%20dc (accessed Aug. 23, 2023).
- 27. O. Ellabban and Joeri Van Mierlo, "Comparative Evaluation of PID Voltage Mode, PI Current Mode, Fuzzy and PWM Based Sliding Mode Control for DC-DC Converters," THE THIRTEEN INTERNATIONAL MIDDLE- EAST POWER SYSTEMS CONFERENCE MEPCON'2009, Jan. 2009, Available: https://www.researchgate.net/publication/202018692_Comparative_Evaluation_of_PI D_Voltage_Mode_PI_Current_Mode_Fuzzy_and_PWM_Based_Sliding_Mode_Control for DC-DC Converters#fullTextFileContent
- 28. F. C. Korkmaz, M. E. Su, and Fuat Alarçin, "CONTROL OF A SHIP SHAFT TORSIONAL VIBRATION VIA MODIFIED PID CONTROLLER," vol. 65, no. 1, pp. 17–27, Mar. 2014.
- 29. D. Sain, "PID, I-PD and PD-PI controller design for the ball and beam system: A comparative study," vol. 9, no. 39, pp. 9–14, Jan. 2017, Available: https://www.researchgate.net/publication/312083564_PID_I-PD_and_PD-PI_controller_design_for_the_ball_and_beam_system_A_comparative_study

- 30. O. Shiryayeva, Batyrbek Suleimenov, and Y. Kulakova, "Optimal Design of I-PD and PI-D Industrial Controllers Based on Artificial Intelligence Algorithm," Algorithms, vol. 17, no. 7, pp. 288–288, Jul. 2024, doi: https://doi.org/10.3390/a1707028
- 31. D. Guha, P. K. Roy, and S. Banerjee, "Load frequency control of large scale power system using quasi-oppositional grey wolf optimization algorithm," Engineering Science and Technology, an International Journal, vol. 19, no. 4, pp. 1693–1713, Dec. 2016, doi: https://doi.org/10.1016/j.jestch.2016.07.004.
- 32. J.-S. Chou and D.-N. Truong, "A novel metaheuristic optimizer inspired by behavior of jellyfish in ocean," Applied Mathematics and Computation, vol. 389, p. 125535, Jan. 2021, doi: https://doi.org/10.1016/j.amc.2020.125535.
- 33. Daraz, S. A. Malik, H. Mokhlis, I. U. Haq, G. F. Laghari, and N. N. Mansor, "Fitness Dependent Optimizer-Based Automatic Generation Control of Multi-Source Interconnected Power System With Non-Linearities," IEEE Access, vol. 8, pp. 100989–101003, 2020, doi: https://doi.org/10.1109/access.2020.2998127.

Appendix A

Close loop transfer function of PID controller with transfer function 1 is

$$\frac{V_o(s)}{V_{ref}(s)} = \frac{Gc(s)Gp(s)}{1 + Gc(s)Gp(s)}$$
(A-1)

Putting values of $G_C(s)$ and $G_{P1}(s)$ from equation 3.37 and 3.38 in equation A-1

$$\frac{V_0(s)}{V_{ref}(s)} = \frac{216000(Kps + Ki + Kds^2)}{0.0006s^3 + (1 + 216000Kd)s^2 + (6000 + 216000Kp)s + 216000Ki}$$
(A-2)

Formulation for fitness function of PID controller for Case-I

$$E(s) = Vref(s) - Vo(s)$$
 (A-3)

$$Vref(s) = \frac{1}{s}$$
 (A-4)

$$\frac{\text{Vo(s)}}{\text{Vref(s)}} = \frac{216000(\text{Kps+Ki+Kds}^2)}{0.0006\text{s}^3 + (1 + 216000\text{Kd})\text{s}^2 + (6000 + 216000\text{Kp})\text{s} + 216000\text{Ki}}$$
(A-5)

$$Vo(s) = Vref(s) \frac{216000(Kps + Ki + Kds^2)}{0.0006s^3 + (1 + 216000Kd)s^2 + (6000 + 216000Kp)s + 216000Ki}$$
 (A-6)

$$Vo(s) = \frac{1}{s} \left[\frac{216000(Kps + Ki + Kds^2)}{0.0006s^3 + (1 + 216000Kd)s^2 + (6000 + 216000Kp)s + 216000Ki} \right]$$
(A-7)

Now putting A-4 and A-5 in equation A-3

$$E(s) = \frac{1}{s} - \frac{1}{s} \left[\frac{216000(Kps + Ki + Kds^2)}{0.0006s^3 + (1 + 216000Kd)s^2 + (6000 + 216000Kp)s + 216000Ki} \right]$$
(A-8)

$$E(s) = \frac{1}{s} \left[1 - \frac{216000(Kps + Ki + Kds^2)}{0.0006s^3 + (1 + 216000Kd)s^2 + (6000 + 216000Kp)s + 216000Ki} \right]$$
(A-9)

$$E(s) =$$

$$\frac{1}{s} \left[\frac{0.0006s^3 + (1 + 216000 \text{Kd})s^2 + (6000 + 216000 \text{Kp})s + 216000 \text{Ki} - 216000 (\text{Kps} + \text{Ki} + \text{Kds}^2)}{0.0006s^3 + (1 + 216000 \text{Kd})s^2 + (6000 + 216000 \text{Kp})s + 216000 \text{Ki}} \right] (\text{A}10)$$

$$E(s) = \frac{1}{s} \left[\frac{0.0006s^3 + s^2 + 6000s}{0.0006s^3 + (1 + 216000Kd)s^2 + (6000 + 216000Kp)s + 216000Ki} \right]$$
(A-11)

$$E(s) = \left[\frac{0.0006s^2 + s + 6000}{0.0006s^3 + (1 + 216000 \text{Kd})s^2 + (6000 + 216000 \text{Kp})s + 216000 \text{Ki}} \right]$$
(A-12)

e(t) = 3 * symsum((r3 * exp(r3 * t)) / (1080000000 * Kp + 9 * r3^2 + 21600000000 * Kd * r3 + 10000 * r3 + 30000000), k, 1, 3) + 5000 * symsum((r3* exp(r3 * t)) / (1080000000 * Kp + 10000 * r3 + 9 * r3^2 + 2160000000 * Kd * r3 + 3000000), k, 1, 3) + 30000000 * symsum(exp(r3 * t) / (1080000000 * Kp + 9 * r3^2 + 2160000000) * Kd * r3 + 10000 * r3 + 30000000), k, 1, 3);

Where, $r3 = root(s3^3 + 360000000*Kd*s3^2 + (5000*s3^2)/3 + 360000000*Kp*s3+ 100000000*s3+ 360000000*Ki, s3, k);$

Appendix B

Close loop transfer function of I-PD controller with transfer function 1 is

$$\frac{V_o(s)}{V_{ref}(s)} = \frac{Gc(s)Gp(s)}{1+Gc(s)Gp(s)}$$
(B-1)

Putting values of $G_C(s)$ and $G_{P1}(s)$ from equation 3.37 and 3.39 in equation A-1

$$\frac{V_0(s)}{V_{ref}(s)} = \frac{1280(Kps + Ki + Kds^2)}{8e - 8s^3 + (0.0001 + 1280Kd)s^2 + (8 + 1280Kp)s + 1280Ki}$$
(B-2)

Formulation for fitness function of PID controller for Case-II

$$E(s) = Vref(s) - Vo(s)$$
(B-3)

$$Vref(s) = \frac{1}{s}$$
 (B-4)

$$\frac{\text{Vo(s)}}{\text{Vref(s)}} = \frac{1280(\text{Kps+Ki+Kds}^2)}{8e-8s^3+(0.0001+1280\text{Kd})s^2+(8+1280\text{Kp})s+1280\text{Ki}}$$
(B-5)

$$Vo(s) = Vref(s) \frac{1280(Kps + Ki + Kds^2)}{8e - 8s^3 + (0.0001 + 1280Kd)s^2 + (8 + 1280Kp)s + 1280Ki}$$
(B-6)

Now putting B-4 and B-5 in equation B-3

$$E(s) = \frac{1}{s} - \frac{1}{s} \left[\frac{1280(Kps + Ki + Kds^2)}{8e - 8s^3 + (0.0001 + 1280Kd)s^2 + (8 + 1280Kp)s + 1280Ki} \right]$$
(B-7)

$$E(s) = \frac{1}{s} \left[1 - \frac{1280(Kps + Ki + Kds^2)}{8e - 8s^3 + (0.0001 + 1280Kd)s^2 + (8 + 1280Kp)s + 1280Ki} \right]$$
(B-8)

$$E(s) = \frac{1}{s} \left[\frac{8e - 8s^3 + (0.0001 + 1280 \text{Kd})s^2 + (8 + 1280 \text{Kp})s + 1280 \text{Ki} - 1280 (\text{Kps} + \text{Ki} + \text{Kds}^2)}{8e - 8s^3 + (0.0001 + 1280 \text{Kd})s^2 + (8 + 1280 \text{Kp})s + 1280 \text{Ki}} \right] (B-9)$$

$$E(s) = \frac{1}{s} \left[\frac{8e - 8s^3 + 0.0001s^2 + 8s}{8e - 8s^3 + (0.0001 + 1280 \text{Kd})s^2 + (8 + 1280 \text{Kp})s + 1280 \text{Ki}} \right]$$
(B-10)

$$E(s) = \left[\frac{8e - 8s^2 + 0.0001s + 8}{8e - 8s^3 + (0.0001 + 1280 \text{Kd})s^2 + (8 + 1280 \text{Kp})s + 1280 \text{Ki}} \right]$$
(B-11)

```
e(t) = 2361183241434822606848 * symsum((exp(root f(k) * t) * root f(k)^2) / denom1, k, 1, 3) +
1888946593147858125 * symsum((exp(root_f(k) * t) * root_f(k)) / denom2, k, 1, 3) +
188894659314785808547840000 * symsum(exp(root f(k) * t) / denom3, k, 1, 3);
where
root f = (a/k) root(polynomial, s15, k);
denom1 = 30223145490365729367654400000*Kp + 4722366482869645213696*root f(k) + 47223664828696*root f(k) + 4722366482869645213696*root f(k) + 47223664828696*root f(k) + 472236648286968696*root f(k) + 47223664828696*root f(k) + 472236668686*root f(k) + 47223668686*root f(k) + 4722366688696*root f(k) + 47223668686868696*root f(k
5666839779443574375*root f(k)^2
                                                                                                                              60446290980731458735308800000*Kd*root f(k)
188894659314785808547840000;
denom2
                                                                                                                      30223145490365729367654400000*Kp
                                                                                                                                                                                                                                                                                      +
60446290980731458735308800000*Kd*root f(k) +
                                                                                                                                                                      5666839779443574375*root f(k)^2
                                                                                                                                                                                                                                                                                      +
4722366482869645213696*root f(k) + 188894659314785808547840000;
denom3
                                                                                                                      30223145490365729367654400000*Kp
                                                                                                                                                                                                                                                                                      +
60446290980731458735308800000*Kd*root f(k) +
                                                                                                                                                                      5666839779443574375*root f(k)^2
4722366482869645213696*root f(k) + 188894659314785808547840000;
```

Appendix C

Close loop transfer function of I-PD controller with transfer function 1 is

$$\frac{V_o(s)}{V_{ref}(s)} = \frac{Gc(s)Gp(s)}{1+Gc(s)Gp(s)}$$
(C-1)

Putting values of $G_{\mathbb{C}}(s)$ and $G_{\mathbb{P}1}(s)$ from equation 3.44 and 3.45 in equation A-1

$$\frac{V_0(s)}{V_{ref}(s)} = \frac{216000 \text{Ki}}{6e - 4s^3 + (1 + 216000 \text{Kd})s^2 + (6000 + 216000 \text{Kp})s + 2160000 \text{Ki}}$$
(C-2)

Formulation for fitness function of I-PD controller for Case-I

$$E(s) = Vref(s) - Vo(s)$$
 (C-3)

$$Vref(s) = \frac{1}{s}$$
 (C-4)

$$\frac{\text{Vo(s)}}{\text{Vref(s)}} = \frac{216000\text{Ki}}{0.0006\text{s}^3 + (1 + 216000\text{Kd})\text{s}^2 + (6000 + 216000\text{Kp})\text{s} + 216000\text{Ki}}$$
(C-5)

$$Vo(s) = Vref(s) \left[\frac{216000Ki}{0.0006s^3 + (1 + 216000Kd)s^2 + (6000 + 216000Kp)s + 216000Ki} \right] (C-6)$$

$$Vo(s) = \frac{1}{s} \left[\frac{216000 \text{Ki}}{0.0006 \text{s}^3 + (1 + 216000 \text{Kd}) \text{s}^2 + (6000 + 216000 \text{Kp}) \text{s} + 216000 \text{Ki}}} \right]$$
 (C-6)

Now putting C-4 and C-5 in equation C-3

$$E(s) = \frac{1}{s} - \frac{1}{s} \left[\frac{216000 \text{Ki}}{0.0006 \text{s}^3 + (1 + 216000 \text{Kd}) \text{s}^2 + (6000 + 216000 \text{Kp}) \text{s} + 216000 \text{Ki}}} \right] \quad \text{(C-7)}$$

$$E(s) = \frac{1}{s} \left[1 - \frac{216000 \text{Ki}}{0.0006 s^3 + (1 + 216000 \text{Kd}) s^2 + (6000 + 216000 \text{Kp}) s + 216000 \text{Ki}} \right] \quad \text{(C-8)}$$

$$E(s) = \frac{1}{s} \left[\frac{0.0006s^3 + (1 + 216000 \text{Kd})s^2 + (6000 + 216000 \text{Kp})s + 216000 \text{Ki} - 216000 \text{Ki})}{0.0006s^3 + (1 + 216000 \text{Kd})s^2 + (6000 + 216000 \text{Kp})s + 216000 \text{Ki}} \right] (C-9)$$

$$E(s) = \frac{1}{s} \left[\frac{0.0006s^3 + (1 + 216000 \text{Kd})s^2 + (6000 + 216000 \text{Kp})s}{0.0006s^3 + (1 + 216000 \text{Kd})s^2 + (6000 + 216000 \text{Kp})s + 216000 \text{Ki}} \right]$$
(C-10)

$$E(s) = \left[\frac{0.0006s^2 + (1 + 216000 \text{Kd})s + (6000 + 216000 \text{Kp})}{0.0006s^3 + (1 + 216000 \text{Kd})s^2 + (6000 + 216000 \text{Kp})s + 216000 \text{Ki}} \right]$$
(C-11)

Appendix D

Close loop transfer function of I-PD controller with transfer function 1 is

$$\frac{V_0(s)}{V_{ref}(s)} = \frac{Gc(s)Gp(s)}{1+Gc(s)Gp(s)}$$
(D-1)

Putting values of $G_C(s)$ and $G_{P1}(s)$ from equation 3.44 and 3.46 in equation A-1

$$\frac{V_0(s)}{V_{ref}(s)} = \frac{1280Ki}{8e - 8s^3 + (0.0001 + 1280Kd)s^2 + (8 + 1280Kp)s + 1280Ki}$$
(D-2)

Formulation for fitness function of I-PD controller for transfer function 2

$$E(s) = Vref(s) - Vo(s)$$
 (D-3)

$$Vref(s) = \frac{1}{s}$$
 (D-4)

$$\frac{\text{Vo(s)}}{\text{Vref(s)}} = \frac{1280\text{Ki}}{8e - 8s^3 + (0.0001 + 1280\text{Kd})s^2 + (1280 + 8\text{Kp})s + 1280\text{Ki}}$$
(D-5)

$$Vo(s) = Vref(s) \left[\frac{1280Ki}{8e - 8s^3 + (0.0001 + 1280Kd)s^2 + (1280 + 8Kp)s + 1280Ki} \right]$$
 (D-6)

$$Vo(s) = \frac{1}{s} \left[\frac{1280 \text{Ki}}{8e - 8s^3 + (0.0001 + 1280 \text{Kd})s^2 + (1280 + 8 \text{Kp})s + 1280 \text{Ki}} \right]$$
(D-7)

Now putting D-4 and D-5 in equation D-3

$$E(s) = \frac{1}{s} - \frac{1}{s} \left[\frac{1280 \text{Ki}}{8e - 8s^3 + (0.0001 + 1280 \text{Kd})s^2 + (1280 + 8 \text{Kp})s + 1280 \text{Ki}} \right]$$
(D-8)

$$E(s) = \frac{1}{s} \left[1 - \frac{1280 \text{Ki}}{8e - 8s^3 + (0.0001 + 1280 \text{Kd})s^2 + (1280 + 8 \text{Kp})s + 1280 \text{Ki}} \right]$$
(D-9)

$$E(s) = \frac{1}{s} \left[\frac{8e - 8s^3 + (0.0001 + 1280 \text{Kd})s^2 + (1280 + 8\text{Kp})s + 1280 \text{Ki} - 1280 \text{Ki}}{8e - 8s^3 + (0.0001 + 1280 \text{Kd})s^2 + (1280 + 8\text{Kp})s + 1280 \text{Ki}} \right]$$
(D-10)

$$E(s) = \frac{1}{s} \left[\frac{8e - 8s^3 + (0.0001 + 1280 \text{Kd})s^2 + (1280 + 8\text{Kp})s}{8e - 8s^3 + (0.0001 + 1280 \text{Kd})s^2 + (1280 + 8\text{Kp})s + 1280 \text{Ki}} \right]$$
(D-11)

$$E(s) = \left[\frac{8e - 8s^2 + (0.0001 + 1280 \text{Kd})s + (1280 + 8Kp)}{8e - 8s^3 + (0.0001 + 1280 \text{Kd})s^2 + (1280 + 8Kp)s + 1280 \text{Ki}} \right]$$
(D-12)

```
e(t) = 30223145490365729367654400000 * Kd * symsum((root_f(k) * exp(root_f(k) * t)) / denom1, \\ k, 1, 3) + ... 2361183241434822606848 * symsum((root_f(k) * exp(root_f(k) * t)) / denom2, k, 1, 3) \\ + ... 188894659314785808547840000 * symsum(exp(root_f(k) * t) / denom3, k, 1, 3); \\ root_f = @(k) root(polynomial, s15, k); \\ denom1 = 30223145490365729367654400000*Kp + 4722366482869645213696*root_f(k) + \\ 5666839779443574375*root_f(k)^2 + 60446290980731458735308800000*Kd*root_f(k) + \\ 188894659314785808547840000; \\ denom2 = 30223145490365729367654400000*Kp + \\ 60446290980731458735308800000*Kd*root_f(k) + ... 5666839779443574375*root_f(k)^2 + \\ 4722366482869645213696*root_f(k) + 188894659314785808547840000; \\ denom3 = 30223145490365729367654400000*Kp + \\ 60446290980731458735308800000*Kd*root_f(k) + 5666839779443574375*root_f(k)^2 + \\ 4722366482869645213696*root_f(k) + 188894659314785808547840000; \\ denom3 = 30223145490365729367654400000*Kp + \\ 60446290980731458735308800000*Kd*root_f(k) + 5666839779443574375*root_f(k)^2 + \\ 4722366482869645213696*root_f(k) + 188894659314785808547840000; % \\ \end{cases}
```